CRMP-1 enhances EVL-mediated actin elongation to build lamellipodia and the actin cortex

Hui-Chia Yu-Kemp, James P. Kemp Jr., and William M. Brieher

Department of Cell and Developmental Biology, University of Illinois, Urbana-Champaign, IL

Cells can control actin polymerization by nucleating new filaments or elongating existing ones. We recently identified CRMP-1 as a factor that stimulates the formation of *Listeria monocytogenes* actin comet tails, thereby implicating it in actin assembly. We now show that CRMP-1 is a major contributor to actin assembly in epithelial cells, where it works with the Ena/VASP family member EVL to assemble the actin cytoskeleton in the apical cortex and in protruding lamellipodia. CRMP-1 and EVL bind to one another and together accelerate actin filament barbed-end elongation. CRMP-1 also stimulates actin assembly in the presence of VASP and Mena in vitro, but CRMP-1–dependent actin assembly in MDCK cells is EVL specific. Our results identify CRMP-1 as a novel regulator of actin filament elongation and reveal a surprisingly important role for CRMP-1, EVL, and actin polymerization in maintaining the structural integrity of epithelial sheets.

Introduction

Actin polymerization is necessary for a wide range of cellular processes, including cell motility and cell shape change. Even stationary cells such as those within interconnected sheets of epithelial cells require continuous actin polymerization, not only for membrane dynamics such as endocytosis, but also to maintain actin-dependent adhesive junctions and repair breaches in the epithelial barrier that are likely to occur from normal wear and tear (Marchiando et al., 2010; Tang and Brieher, 2013; Enyedi and Niethammer, 2015). Hence, the physiological function of both highly motile and relatively sessile cells requires continuous actin polymerization.

Cells generate actin polymer either by nucleating new filaments de novo from G-actin subunits or by elongating existing filaments. Both nucleation and elongation are highly regulated and are under the control of different factors. The Arp2/3 complex, for example, is an important actin nucleation factor whose activity is controlled by a long list of nucleation-promoting factors such as N-WASP, Scar/WAVE, and others that activate Arp2/3 at specific cellular locations at specified times (Welch and Mitchison, 1998; Machesky et al., 1999; Goley and Welch, 2006). Arp2/3-dependent nucleation reactions are most frequently associated with motility. Arp2/3-dependent actin nucleation reactions are important for intracellular motility of pathogens including the propulsion of *Listeria monocytogenes*, *Shigella flexneri*, *Rickettsia*, and *Vaccinia* (Welch et al., 1998; Egile et al., 1999; Frischknecht et al., 1999; Loisel et al., 1999; Yarar et al., 1999; Jeng et al., 2004; Weisswange et al., 2009; Welch and Way, 2013), as well as the actin-dependent propulsion of endosomes and internalization of phagosomes (Moreau et al., 1997; May et al., 2000; Duncan et al., 2001; Derivery et al., 2009). Arp2/3 is also crucial for the formation of lamellipodia that push the leading edge of migrating cells forward (Welch et al., 1997; Suraneni et al., 2012). Beyond these well-established roles for Arp2/3 in motility, the complex also contributes to the assembly of actin networks in nonmotile cells, where it is important for the assembly of actin at cadherin-mediated cell–cell junctions (Verma et al., 2004, 2012; Abu Taha et al., 2014).

Ena/VASP family proteins Ena, VASP, and Ena/VASP-like protein (EVL), on the other hand, are a family of actin-elongation factors that promote the growth of the barbed ends of existing actin filaments (Bear and Gertler, 2009). These factors can increase the rate at which filament barbed ends elongate (Hansen and Mullins, 2010; Breitsprecher et al., 2011; Winkelman et al., 2014), and they help shield the growing barbed end from termination by capping protein (Bear et al., 2002; Barzik et al., 2005). Inside the cell, VASP family proteins often localize to Arp2/3-dependent structures, including lamellipodia (Rottner et al., 1999), and at cell–cell contacts (Vasioukhin et al., 2000; Scott et al., 2006). Ena/VASP proteins can even promote Arp2/3-dependent actin assembly by binding to WAVE (Havrylenko et al., 2015). Cells contain several Ena/VASP binding partners that presumably help localize these elongation factors to specific sites in cells (Bear and Gertler, 2009). Lamellipodin, for example, is important for localizing VASP to the leading edge of lamellipodia, where VASP helps polymerize actin to push the leading edge

Correspondence to William M. Brieher: wbrieher@illinois.edu

The Rockefeller University Press
J. Cell Biol. Vol. 216 No. 8 2463–2479
https://doi.org/10.1083/jcb.201606084

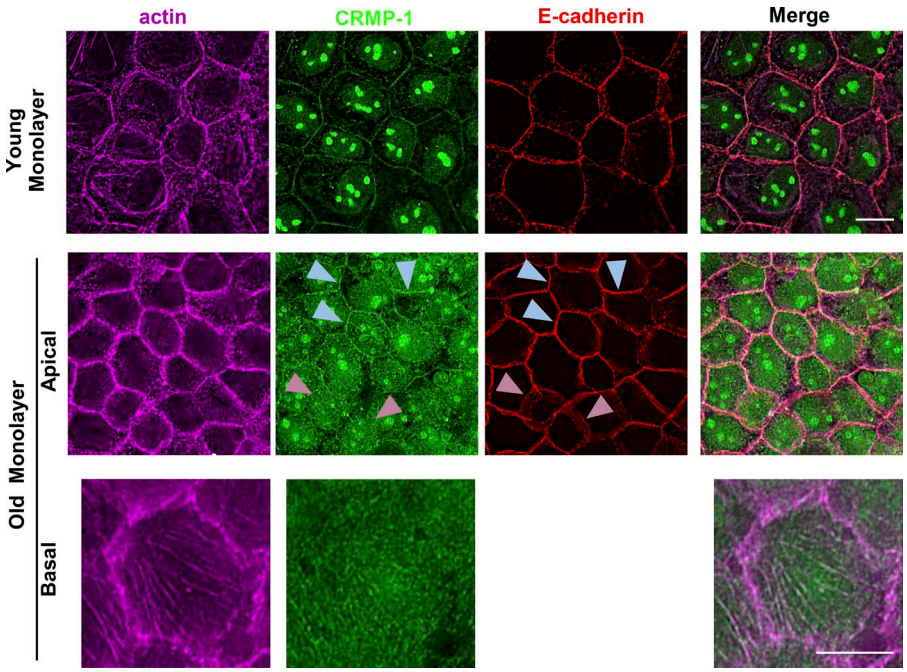

Figure 1. **CRMP-1 is expressed in MDCK cells and localizes to junctional and cortical actin.** Immunostaining of confluent monolayers of MDCK cells showing that CRMP-1 (green) localizes with actin (purple) at cell–cell contacts, which are marked with E-cadherin (red). CRMP-1 signal at this location can be detected in the apical surface of the young monolayer (day 1 of confluence; top) and the old monolayer (day 6 of confluence; middle), but not at the lateral membrane. Blue arrowheads, apical membrane; pink arrowheads, lateral membrane. CRMP-1 can be detected at the basal surface of the cell, yet its signal does not colocalize with any specific actin structures (bottom). Bars, 10 µm.

forward (Krause et al., 2004; Hansen and Mullins, 2015). Thus far, however, lamellipodin and profilin are the only proteins known to stimulate the elongation activity of Ena/VASP proteins (Hansen and Mullins, 2010). Because actin assembly is so heavily regulated, it is likely that additional factors and mechanisms controlling actin polymerization remain to be identified.

We recently identified CRMP-1 as a novel factor that promotes Arp2/3-dependent assembly of *Listeria* actin comet tails (Yu-Kemp and Brieher, 2016). *Listeria* is an intracellular bacterial pathogen that recruits proteins from the eukaryotic host to build the actin comet tail that propels the pathogen through the host's cytoplasm and to adjacent cells to spread the infection (Welch et al., 1997; Loisel et al., 1999; Brieher et al., 2004). CRMP-1 is one member of a family of five related proteins implicated in a variety of cytoskeleton-dependent processes such as neuronal growth cone motility and collapse, neuronal polarity, endocytosis, and the anchoring of ion channels in the plane of the membrane. (Li et al., 1992; Goshima et al., 1995; Arimura et al., 2000; Inagaki et al., 2001; Shih et al., 2001; Fukata et al., 2002; Brittain et al., 2009; Maniar et al., 2011). The molecular mechanisms through which CRMP proteins mediate these processes are still mysterious. One popular model is that CRMP binds to tubulin to promote microtubule assembly (Fukata et al., 2002; Lin et al., 2011; Khazaei et al., 2014). Other studies suggest that CRMPs might promote or inhibit actin filament bundling (Rosslenbroich et al., 2005; Nakamura et al., 2014). Our results with *Listeria* implicate CRMP-1 in actin assembly (Yu-Kemp and Brieher, 2016).

Our goals in this study were to determine whether CRMP-1 contributes to actin network formation outside of *Listeria* actin comet tails and, if so, to identify a possible underlying mechanism. We found that MDCK cells express CRMP-1, providing a simple model system for studying CRMP-1 function in organizing actin in an established, nontransformed kidney epithelial cell line.

Results

CRMP colocalizes with actin in confluent monolayers of MDCK cells

We sought to characterize the distribution of CRMP-1 in MDCK cells, which would provide a simple system to study the possible role of CRMP-1 in cellular actin assembly. To do so, we first performed immunostaining with a CRMP-1 antibody and phalloidin to visualize the relative cellular locations of CRMP-1 and actin. MDCK is an epithelial cell line that forms cadherin-dependent cell–cell adhesions once the cells contact each other. Therefore, we also stained for E-cadherin to mark the cell border. In a young MDCK monolayer that had been at confluence for 1 d, we detected CRMP-1 colocalizing with actin and E-cadherin at cell borders at this stage (Fig. 1, top).

As MDCK monolayers age, the cells become more polarized and taller, and the junctions mature and become more stable. To determine whether CRMP-1 also localized to the same cellular localizations after the cells polarized, we performed the same staining on a mature monolayer that had been at confluence for 6 d. Unlike the young monolayer, which is thin enough that most of the actin could be imaged in a single optical plane (Fig. 1, top), the mature monolayer has a height of ∼2.5 µm. At the apical surface, actin filaments concentrated at cell borders. At the basal surface, actin filaments were in stress fibers. Under this condition, CRMP-1 localized with actin at cell borders, where it still concentrated with E-cadherin and actin near apical cell–cell junctions, but not at the lateral membrane (Fig. 1, middle, apical view). In contrast, CRMP-1 did not concentrate at cell borders near the basal surface of the cell (Fig. 1, bottom, basal view). In addition, a strong CRMP-1 signal was present inside the cell in these aged monolayers, which corresponded to the cortical actin network beneath the apical and basal surfaces of the cell. Note that the intense nucleolar staining is not specific, because we still see it in the cells depleted of CRMP-1 (Fig. S1). CRMP-1 periodically showed some lo-

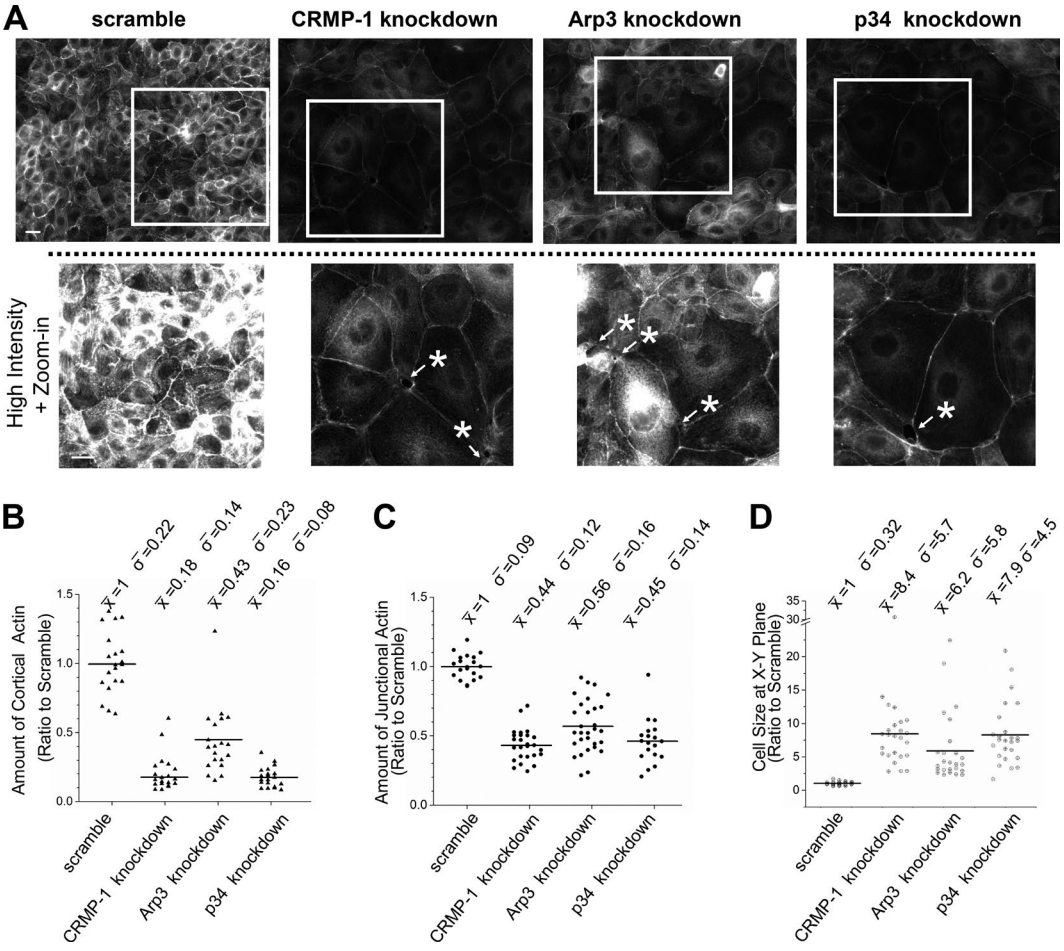

Figure 2. **Perturbing CRMP-1 or Arp2/3 function results in the loss of cortical actin and junctional actin.** (A) Actin staining in confluent MDCK monolayers of control cells (scramble) and knockdown cells (CRMP-1, Arp3, or p34 knockdown). White stars indicate the holes detected in a confluent monolayer. Bars, 20 µm. (B–D) Quantification of A. Amounts of cortical actin (B) and junctional actin (C) decreased in the knockdown cells. For quantification, $n \geq 20$. (D) Cell size in the *x–y* plane. In this set of measurements, control cells transfected with the scrambled shRNA have a mean area ~400 µm², which was standardized to 1 in the *y* axis. 25 cells were measured in each condition. Each dot represents the quantification result of one cell; horizontal lines indicate the mean of the 25 data points.

calization to basal stress fibers in mature monolayers (Fig. 1, bottom, basal view), even though the localization was not seen in a young monolayer (Fig. 1, top). Together, these staining results indicate that CRMP-1 is expressed and localizes to actin structures in MDCK cells.

CRMP-1 and Arp2/3 assemble the same actin networks

To test whether CRMP-1 contributes to actin assembly and organization, we depleted it from MDCK cells using shRNAs. Western blotting showed that the shRNA depleted CRMP-1 protein (Fig. S2 A). F-actin staining in CRMP-1–depleted cells was diminished relative to control cells transfected with a scrambled shRNA (Fig. 2 A). Quantification of the results showed that the intensity of F-actin in the cortex was reduced relative to controls (Fig. 2 B).

The Arp2/3 complex is thought to be the major actin nucleator responsible for actin assembly at cell junctions and the apical cortex in MDCK cells (Tang and Brieher, 2013), but that study only used drugs to perturb Arp2/3 activity. To better assess whether these actin networks were in fact Arp2/3 dependent, we depleted either Arp3 or the p34 subunit of the Arp2/3 complex using shRNA (Fig. S2, B and C). In both cases, actin accumulation in the cortex was diminished relative to control cells (Fig. 2, A and B). Quantification of the results showed that a reduction in Arp3 or p34 led to a 50% or 50–80% reduction in cortical actin, respectively (Fig. 2, A and B). The actin signal was also reduced at cell–cell borders (Fig. 2 C), which is consistent with a loss in cortical actin in general, but the decrease in actin intensity at cell boundaries in the knockdowns might be the result of a change in cell height.

In addition to the loss of actin, we noticed a significant increase in cell spreading in the plane of the substrate in cells depleted of CRMP-1, p34, or Arp3 (Fig. 2 D). In each case, the areas of depleted cells were five to eight times larger than the areas of control cells. The increase in cell area suggested that the knockdowns might have affected cell volume. We estimated cell volume in rounded cells than had been detached from the substrate by incubation in calcium- and magnesium-free medium. These estimates suggest that knockdown cells are of approximately twice the volume of control cells. The increase in cell volume might be accompanied by an increase in nuclear size. Certainly, the area of the nucleus in these flat cells was twofold higher than that in control cells (Fig. S3). A more detailed analysis will have to be performed to understand the possible changes in cell and nuclear size. Nevertheless, the phenotypes

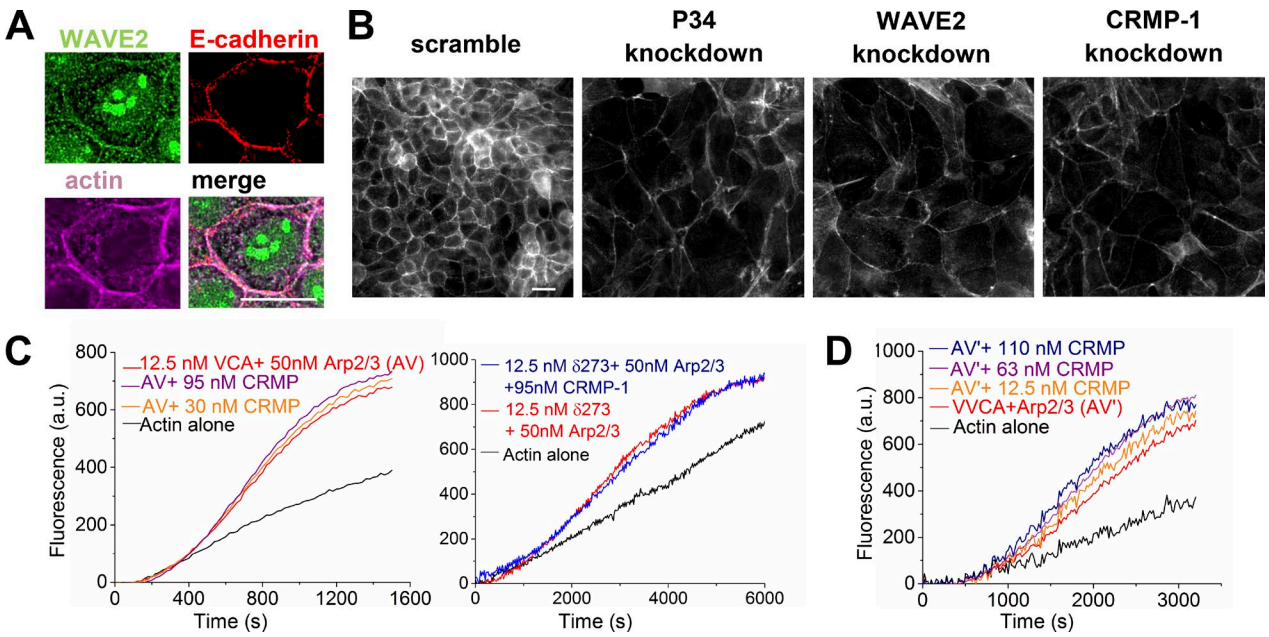

Figure 3. **CRMP-1 does not promote Arp2/3-dependent polymerization in the presence of canonical activators.** (A) WAVE2 (green) localized to cell boundaries, marked with E-cadherin (red) and actin (purple) in a confluent MDCK monolayer. Bar, 10 µm. (B) Phalloidin staining reveals that WAVE2 knockdown cells show phenotypes similar to Arp2/3 and CRMP-1 knockdowns. Bar, 10 µm. (C and D) Actin polymerization assays testing the role of CRMP-1 on Arp2/3 reactions. (C) CRMP-1 does not contribute to Arp2/3 polymerization in the presence of constitutively active WAVE truncations. Left, VCA-induced Arp2/3 reaction; right, δ273-induced reaction. The δ273 construct contains VCA and proline-rich domain of WAVE-2. (D) CRMP-1 does not facilitate Arp2/3 polymerization mediated by VVCA of N-WASP.

show that CRMP-1, p34, and Arp3 contribute to the formation of the same actin networks and produce the same cell phenotype of increased cell spreading.

CRMP-1 does not promote WAVE-mediated activation of Arp2/3

Because CRMP-1 promotes Arp2/3-dependent *Listeria* actin comet tail formation, our first hypothesis was that CRMP-1 would also enhance Arp2/3-mediated actin assembly in cells. CRMP-1 does not directly activate Arp2/3 but rather enhances the ability of *Listeria* ActA to activate the Arp2/3 complex (Yu-Kemp and Brieher, 2016). Eukaryotic cells do not have an obvious ActA homolog, but CRMP-1 might work with the known eukaryotic activators of Arp2/3. Previous studies showed that actin assembly at adherens junctions in intestinal epithelial cells depends on Arp2/3 and WAVE2 (Verma et al., 2004, 2012). In MDCK cells, WAVE2 also localizes to cell boundaries (Fig. 3 A). Depletion of WAVE2 with shRNAs (Fig. S2 D) caused a phenotype that is similar to CRMP-1 and Arp2/3 knockdowns: decreased actin accumulation at cell boundaries and increased cell spreading (Fig. 3 B), demonstrating that these three factors contribute to the same actin networks in MDCK cells.

CRMP-1 promotes the ability of *Listeria* ActA to activate Arp2/3 and nucleate actin polymerization. Because ActA is constitutively active, we hypothesized that CRMP-1 would also promote the ability of constitutively active fragments of WAVE to activate Arp2/3. To test for CRMP-1 stimulation of Arp2/3 activation, we used pyrene actin to track actin polymerization with two different constitutively active WAVE constructs (Suetsugu et al., 2001) containing the VCA domain ± the proline-rich domain, as well as the constitutively active VVCA domain of N-WASP. To our surprise, CRMP-1 did not stimulate the ability of any of these nucleation-promoting factors to activate Arp2/3 (Fig. 3, C and D). Therefore, although CRMP-1 can stimulate the ability of ActA, which is a constitutively active nucleation-promoting factor for Arp2/3, it cannot stimulate the ability of constitutively active forms of WAVE or N-WASP to activate Arp2/3.

CRMP-1 works with VASP family proteins to promote actin assembly

We sought another explanation for the severe loss of actin that occurs when CRMP-1 is depleted from cells. Previous studies from our laboratory showed that EVL is necessary for actin assembly off cadherin-enriched junctional membranes (Tang and Brieher, 2013). CRMP-1 is also present on these membranes (Fig. S4). Ena/VASP family proteins including EVL promote actin assembly from actin filament barbed ends (Pasic et al., 2008; Yang and Svitkina, 2011; Winkelman et al., 2014). We therefore tested whether CRMP-1 could enhance actin assembly in the presence of EVL. 1.5-µM solutions of pyrene actin containing 0 or 40 nM EVL were induced to polymerize. After 30 min, either 100 nM CRMP-1 or a compensatory amount of buffer was added to the reactions. CRMP-1 stimulated actin assembly in the presence of EVL, but it had no effect on actin alone (Fig. 4 A). Increasing concentrations of EVL alone had a modest effect on actin assembly, consistent with previous results (Barzik et al., 2005; Hansen and Mullins, 2010; Breitsprecher et al., 2011; Winkelman et al., 2014). Adding 100 nM CRMP-1 to these reactions boosted the assembly rates (Fig. 4 B).

To emphasize the effect of CRMP-1 on EVL-mediated assembly, we calculated and compared the slope in 3-min windows before and after CRMP-1 was added into the reaction. The results showed that CRMP-1 accelerated actin assembly two- to threefold in the presence of EVL but had no effect on actin assembly in the absence of EVL (Fig. 4 B, right). Similarly,

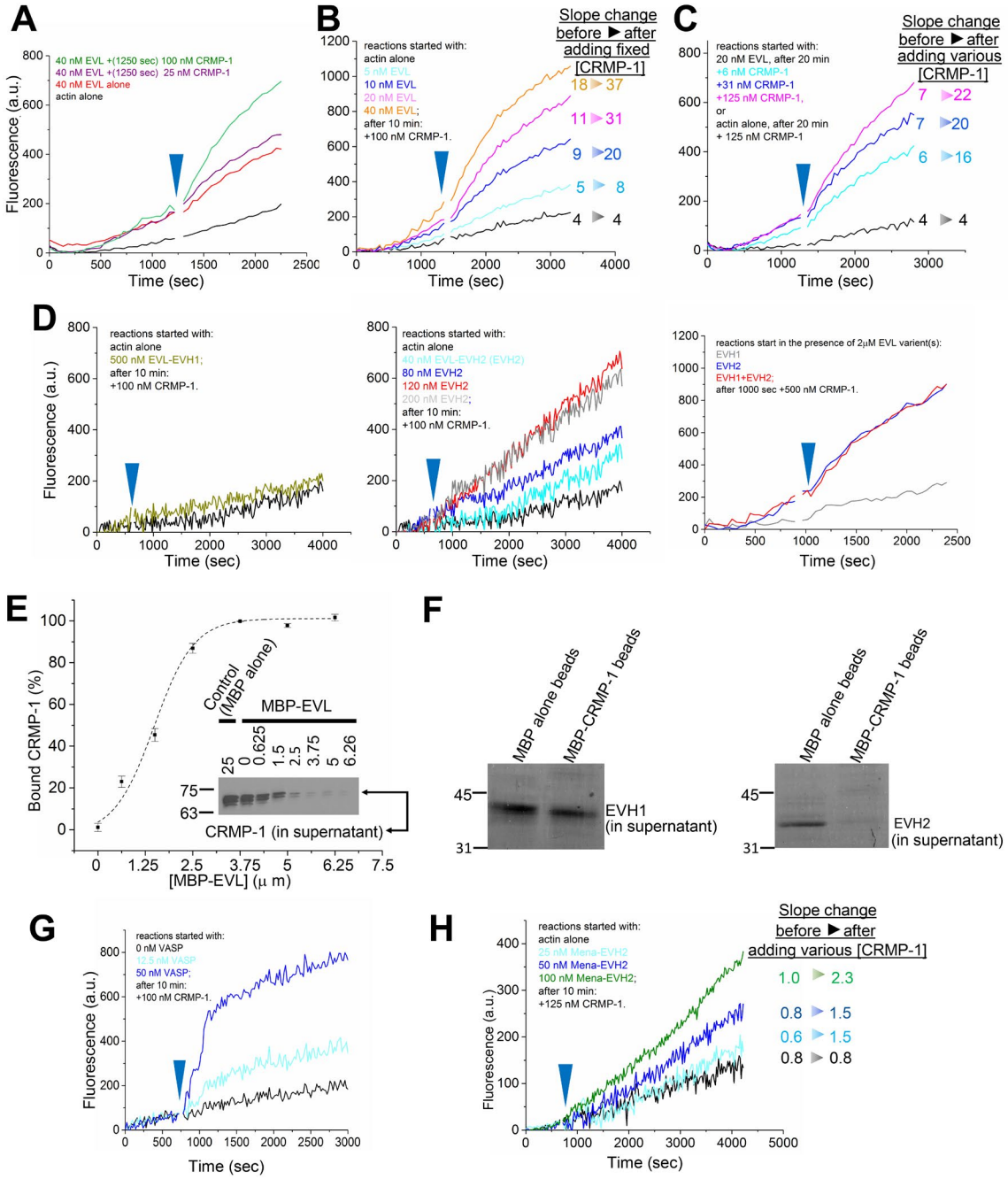

Figure 4. **CRMP-1 works with VASP family proteins to facilitate actin polymerization.** (A) CRMP-1 promotes EVL-mediated actin polymerization. Polymerization was initiated in the presence or absence of 40 nM EVL. 30 min later, either buffer or CRMP-1 was added to the reactions. (B) Actin polymerization was initiated in the presence of increasing concentrations of EVL before adding 100 nM CRMP-1. CRMP-1 enhances EVL-mediated actin polymerization. Right, analysis of the slopes in 3-min window before and after CRMP-1 was added. CRMP-1 induces a two- to threefold increase in polymerization rate. (C) Adding increasing amounts of CRMP-1 to a fixed amount of EVL also provides a dose-dependent effect for actin polymerization. Actin polymerization was initiated with actin alone or 20 nM EVL before adding different concentrations of CRMP-1. (Right) Analysis of the slopes in 3-min window before and after CRMP-1 was added. (D) CRMP-1 promotes actin polymerization with the EVH2 domain, but not the EVH1 domain, of EVL. (E) CRMP-1 interacts with EVL. The binding curve of CRMP-1 to MBP-tagged EVL. Insert, Western blotting of CRMP-1 in the supernatants showing CRMP-1 depletion after incubating with different amounts of EVL. Numbers above each lane indicate total protein concentration on the beads (for concentration, EVL was calculated as tetramer; MBP alone was calculated as monomer). (F) EVH2 of EVL interacts with MBP-tagged CRMP-1, but the EVH1 domain does not. Coomassie staining shows the amount of EVL fragments remaining in the supernatant after incubating with the immobilized MBP or MBP-CRMP-1. (G and H) CRMP-1 contributes to VASP-mediated (G) or MENA-EVH2-mediated (H) actin polymerization. Blue arrowhead indicates when CRMP-1 was added into the reaction.

adding increasing amounts of CRMP-1 to a fixed amount of EVL also showed a dose-dependent increase in the actin assembly rate (Fig. 4 C). Again, CRMP-1 accelerated actin assembly two- to threefold (Fig. 4 C, right). The EVH2 domain of EVL was sufficient to act in concert with CRMP-1 to enhance actin assembly, but the effect was less pronounced than full-length

EVL, whereas the EVH1 domain and CRMP-1 had no effect on actin assembly (Fig. 4 D). These results show that the combination of CRMP-1 and EVL stimulates actin polymerization.

A recent proteomics study identified EVL as a binding partner for CRMP-2 (Martins-de-Souza et al., 2015). Using a pull-down assay, we confirmed that EVL binds directly to CRMP-1 with an affinity of 2 µM (Fig. 4 E). The EVH2 domain of EVL is sufficient for CRMP-1 binding, whereas the EVH1 domain alone failed to bind to CRMP-1 (Fig. 4 F).

In vertebrates, the VASP family consists of three different homologs, VASP, MENA, and EVL, which are generally believed to have redundant biological functions (Menzies et al., 2004; Furman et al., 2007; Kwiatkowski et al., 2007; Takaku et al., 2011). To determine whether CRMP-1 can work with the other VASP family proteins, we repeated the pyrene polymerization experiments with VASP and MENA-EVH2. The results showed that CRMP-1 can facilitate actin polymerization in the presence of VASP or MENA-EVH2 (Fig. 4, G and H).

CRMP-1 facilitates actin elongation with EVL

Previous results have shown that Ena/VASP proteins promote actin elongation, but they can also nucleate actin assembly, at least in vitro (Skoble et al., 2001; Breitsprecher et al., 2011; Winkelman et al., 2014). Our pyrene results showed that CRMP-1 enhances EVL-mediated actin assembly, but the assay cannot distinguish whether CRMP-1 is promoting actin nucleation or elongation in the presence of EVL. To distinguish between these two possibilities, we used widefield fluorescence microscopy to image single filaments polymerizing in the presence or absence of EVL and CRMP-1. We acquired a 3-min time-lapse sequence to record the process of actin polymerization under different conditions.

To determine whether EVL plus CRMP-1 induces any nucleation, we counted the number of filaments in 15 × 15-µm squares over the course of 3 min, comparing actin alone to EVL, CRMP-1, or EVL plus CRMP-1. The micrographs in Fig. 5 A are representative images of actin filaments in each of the four conditions at three different time points. The numbers (N*) below each image are the mean number of filaments found in 10 of such images at that time point. The results show that over the course of 3 min, filament numbers remained within a filament number difference of 1 for all the conditions. Therefore, EVL plus CRMP-1 does not nucleate new actin filaments.

To assess the effects of CRMP-1 and EVL on actin elongation, we compared the lengths of actin filaments at the end of the 3-min video. Adding increasing concentrations of CRMP-1 to actin in the presence of 25 nM EVL produced filaments two to three times longer than those formed by CRMP-1 alone or EVL alone (Fig. 5 B). Because EVL plus CRMP-1 has no effect on actin nucleation (Fig. 5 A), the differences in filament length must be caused by faster elongation rates in the presence of CRMP-1 plus EVL.

Even widefield microscopy provided sufficient contrast to determine actin filament elongation rates from kymographs generated from the time-lapse sequences (Fig. 5 C). This analysis confirmed that the combination of EVL and CRMP-1 accelerated actin filament elongation rates. Actin alone elongated with a rate of 8.4 ± 2.2 subunits/s in our experiment (Fig. 5 D). Neither 60 nM CRMP-1 nor 25 nM EVL/EVH2 alone had any significant effect on the elongation rate (Fig. 5 D). In contrast, the combination of CRMP-1 plus EVL accelerated the elongation rate approximately two- to threefold compared with actin alone. Adding increasing concentrations of CRMP-1 to 1 µM actin and 25 nM EVL accelerated elongation to a maximum rate of ∼18 subunits/s achieved with 100 nM CRMP-1 (∼2.2-fold increase compared with actin alone; Fig. 5 E, top). Similarly, adding increasing amounts of EVL to 100 nM CRMP-1 in the reaction increased the elongation rate two- to threefold compared with EVL alone (Fig. 5 E, bottom), confirming that CRMP-1 augments EVL-dependent actin elongation. Note that CRMP-1 had no effect on how much EVL is required to saturate the reaction. The half-maximal rate of elongation was attained with ∼35 nM EVL in both the absence and presence of CRMP-1. CRMP-1 also accelerates the elongation rate with the EVH2 domain of EVL. The rates saturate at the same concentration of CRMP-1 (100 nM), and the half-maximal concentrations were also the same (40 nM) as with full-length EVL. However, the maximum rate of elongation was slightly slower for EVH2 than for full-length EVL (15 vs. 19 subunits/s, respectively; Fig. 5 E). The differential enhancement of the elongation rate by full-length EVL and EVH2 was also detected in pyrene polymerization assays (Fig. 4, C and D).

EVL is necessary for the assembly of CRMP-1–dependent actin in MDCK cells

Because CRMP-1 promotes actin elongation mediated by VASP family proteins in vitro, we wished to know whether they contribute to CRMP-1–dependent actin network formation in cells. We first determined which VASP family proteins are expressed in MDCK cells. As determined by Western blotting, MDCK cells express VASP and EVL but not MENA (Fig. S2 E).

The cellular localizations of VASP and EVL are different. In confluent monolayers, EVL and CRMP-1 localized with E-cadherin at cell boundaries (Fig. 6 A). EVL localization to cell boundaries was expected, given its association with junction-enriched plasma membranes isolated from liver (Tang and Brieher, 2013). We did not detect VASP at cell boundaries. Instead, VASP is diffuse in the cytoplasm (Fig. 6 B).

We determined the role of EVL and VASP in organizing actin in MDCK cells by depleting them using shRNA. Western blotting shows that the shRNAs specifically targeted either EVL or VASP and did not trigger any compensatory up-regulation of the other family members (Fig. 6 C). Depletion of EVL produced the same phenotype as depleting CRMP-1, including a decrease in junctional and cortical actin and an increase in cell spreading in the plane of the substrate (Fig. 6, D and E). In contrast, depleting VASP did not result in any obvious change in junctional or cortical actin, nor did it alter cell spreading (Fig. 6 F). Overexpressing VASP did not rescue actin accumulation at cell junctions or in the cortex, nor did VASP rescue cell spreading in EVL-depleted cells. Cells expressing VASP in an EVL-depleted background produced more actin stress fibers at the basal surface than cells just depleted of EVL (Fig. 6 G), a result that has been seen before in endothelial cells from Ena/VASP/EVL triple knockout mice overexpressing VASP (Furman et al., 2007). Therefore, although both EVL and VASP can both work with CRMP-1 to enhance actin assembly in vitro, only EVL contributes to CRMP-1–dependent actin structures in confluent monolayers of MDCK cells.

CRMP-1 and EVL are crucial for lamellipodia formation in MDCK cells

These results demonstrated that CRMP-1 and EVL are important for actin assembly in stationary MDCK cells at confluence.

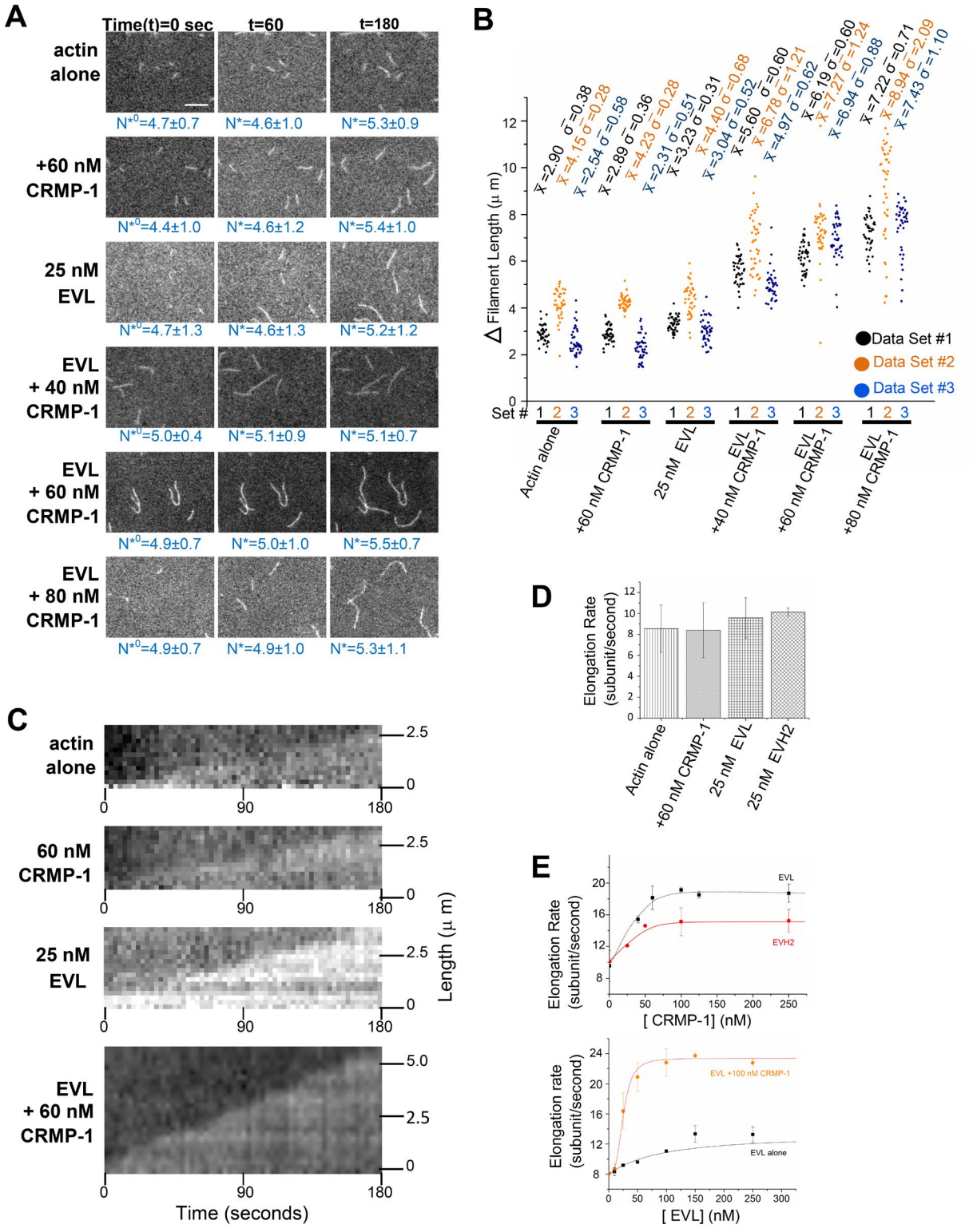

Figure 5. **CRMP-1 accelerates EVL-dependent actin elongation.** (A) Representative images for filament growth under different conditions. N*, mean number of filaments in 15 × 15-μm squares at the indicated time points. Bar, 5 μm. (B) Change in filament length under different conditions over 3 min. Reactions that contain EVL + CRMP-1 made longer filaments after 3 min compared with controls (actin alone, CRMP-1 alone, and EVL alone). *x* axis, different sets of experiments in different conditions; *y* axis, change in filament length from 0 to 3 min. Each dot is one filament. (C) Representative kymographs showing faster elongation in the presence of CRMP-1 and EVL. *x* axis, time (seconds); *y* axis, length (micrometers). (D) Rate of actin filament growth under different conditions. CRMP-1, EVL, or EVH2 alone does not significantly increase the elongation rate. (E) CRMP-1 shows a dose-dependent effect on EVL-mediated elongation. (Top) Increasing amounts of CRMP-1 were added to a fixed amount of EVL or EVH2 (25 nM). (Bottom) Increasing amounts of EVL were added to a fixed amount of CRMP-1 (100 nM). Points on the graph are mean values ± SD, calculated from three individual experiments.

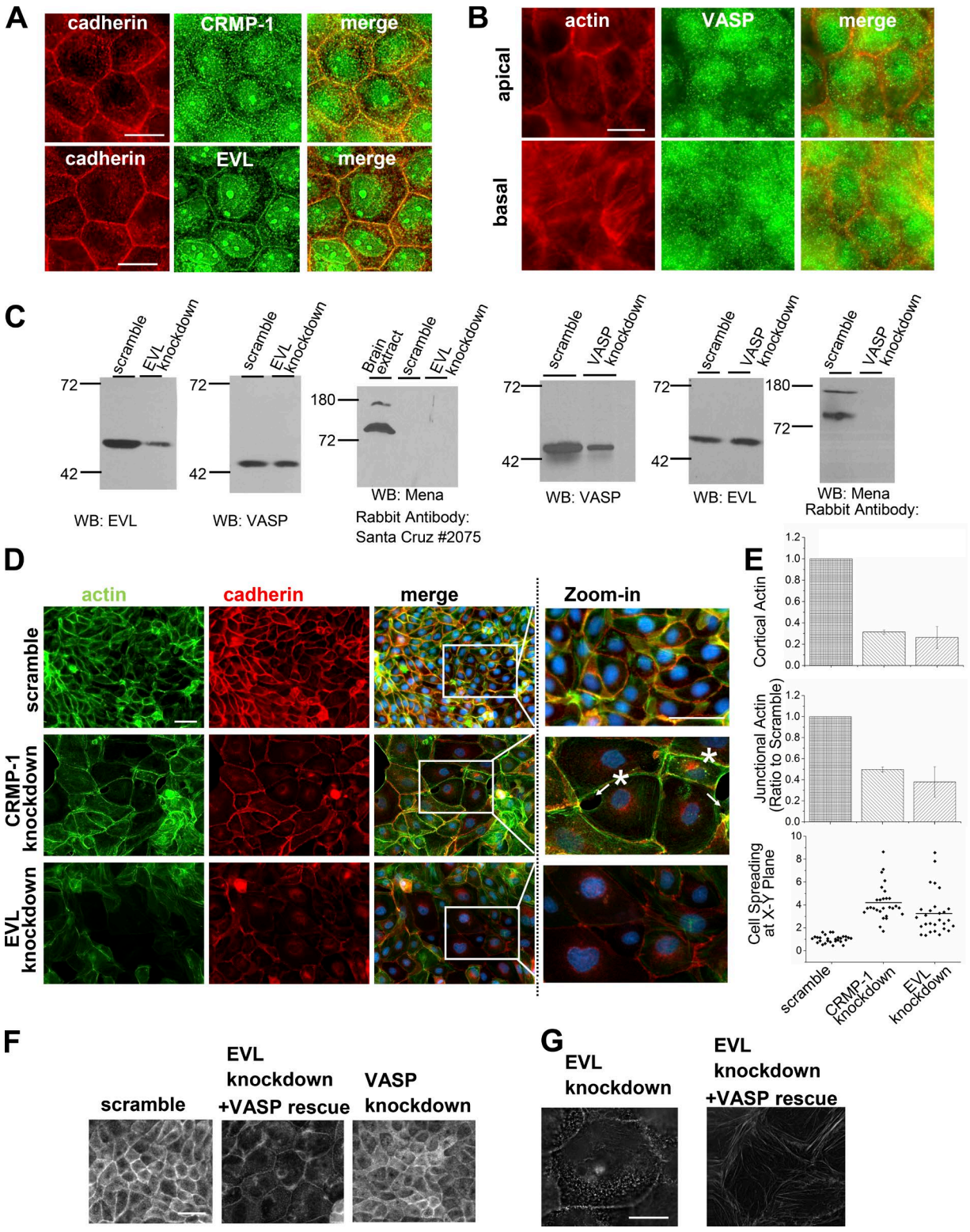

Figure 6. **CRMP-1 and EVL control the amount of actin in MDCK cells.** (A) CRMP-1 and EVL localize to cell–cell borders. Red, cadherin; green, CRMP-1 or EVL. (B) VASP does not show specific localization in a confluent monolayer. Bars, 10 µm. (C) Western blotting confirming the specificity of shRNAs targeting EVL or VASP. (D) Depletion of either CRMP-1 or EVL reduces actin signals in a monolayer. Bars, 20 µm. (E) Quantification of D. Each column represents the mean ± SD from three repeats, each $n = 30$. Dots represents the quantification of each cell. (F and G) Phalloidin staining. (F) Depletion of VASP does not reduce the actin signal or alter cell spreading. Bar, 20 µm. (G) Expression of VASP in EVL-depleted cells induces stress fibers at the basal surface. Bar, 10 µm.

We wished to know whether CRMP-1 contributes to Arp2/3-dependent actin assembly in moving cells. MDCK cells plated on collagen I form lamellipodia in response to wounding. CRMP-1 and EVL localized to these lamellipodia (Fig. 7 A). Cells depleted of either CRMP-1 or EVL did not form lamellipodia, whereas control cells transfected with a scrambled

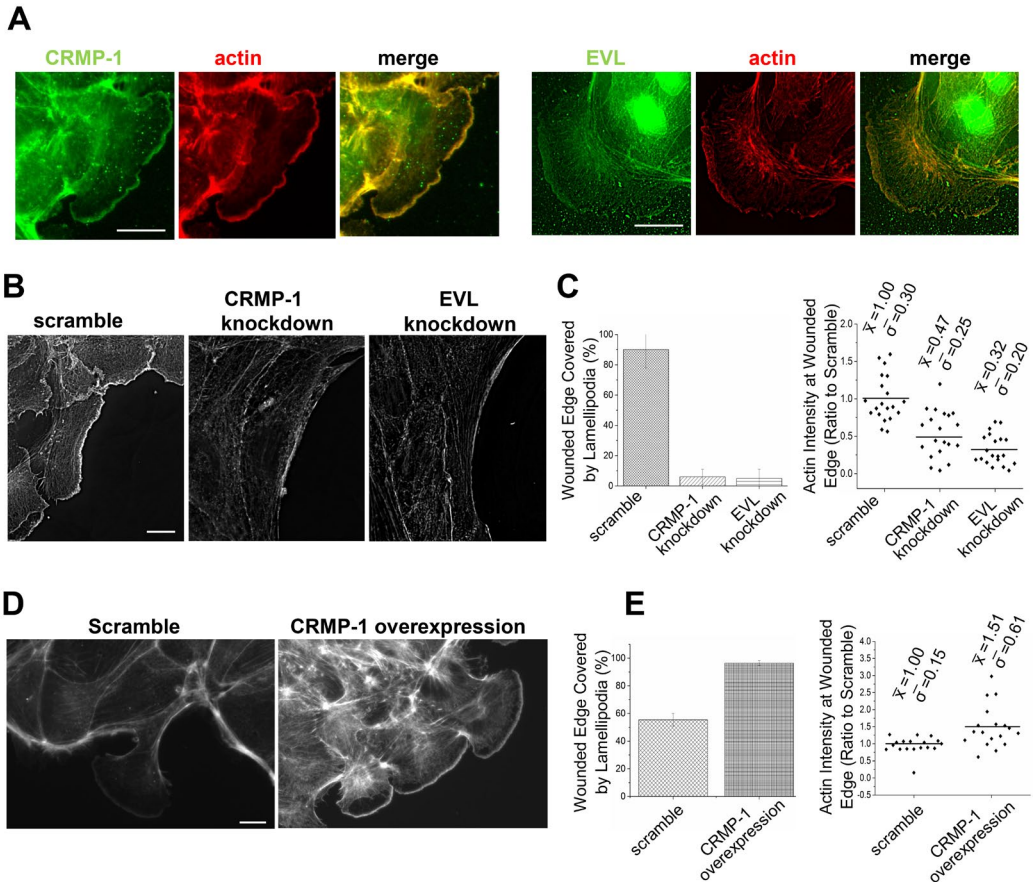

Figure 7. **CRMP-1 and EVL contribute to lamellipodia formation.** (A) Immunostaining showing that CRMP-1 and EVL localize to the leading edge of protruding structures in response to wounding. (B) Phalloidin staining of the wounded edge in scramble or CRMP-1– or EVL-depleted cells. The formation of lamellipodia was perturbed in the knockdown cells. (C) Quantification of B shows that the amounts of lamellipodia and actin at the wound edge are reduced in the knockdown cells. (D) Overexpression of CRMP-1 induces lamellipodia formation. (E) Quantification of D showing that overexpressing CRMP-1 increases the number of lamellipodia and actin intensity at the leading edge in CRMP-1–overexpressing cells compared with control. Column graphs indicate quantifications from three repeats. Dot graphs show the result of one set of the experiments; each dot represent a single data point. Bars, 10 µm. Graphs show the mean ± SD.

shRNA did (Fig. 7 B). Quantification confirmed that more than 80% of control cells at the edge of the wound formed lamellipodia, whereas <10% of cells depleted of CRMP-1 or EVL did (Fig. 7 C, left), and the concentration of F-actin at the wound margin was substantially reduced in cells depleted of either CRMP-1 or EVL (Fig. 7 C, right). Reciprocally, overexpression of CRMP-1 increased the percentage of lamellipodia formation, with increased F-actin detected at the leading edge (Fig. 7 D). In this experiment, we omitted the serum stimulation step that reduces lamellipodia formation in the control condition, allowing a greater range to observe the increase in lamellipodia formation induced by CRMP-1 overexpression.

We next tested the function of VASP in lamellipodia formation in response to wounding. In contrast to EVL, depleting VASP had no obvious effect on lamellipodia formation or the amount of actin in the lamellipodia relative to controls (Fig. 8, A and B). Furthermore, expressing VASP in EVL-depleted cells had only a modest effect on lamellipodia formation. Under these conditions, some cells were able to extend small lamellipodia a short distance into the wound area, but these protruding sheets of membrane were not as robust as the pronounced lamellipodia that formed in control cells (Fig. 8 A, right). VASP does localize to lamellipodia in wild-type cells (Fig. 8 C, yellow arrow), but it does not play as important a role as EVL or CRMP-1 in lamellipodia formation in MDCK cells. VASP also localized to focal adhesions in response to wounding in those cells that did not extend a strong lamellipodia (Fig. 8 C, white arrowhead, and Fig. 8 D). Earlier studies also showed VASP at focal adhesions in other cell types (Haffner et al., 1995; Furman et al., 2007). These results obtained in lamellipodia are consistent with the observations in MDCK monolayers at confluence: EVL is crucial for the formation of CRMP-1–dependent actin networks, but VASP is not.

CRMP-1 contributes to lamellipodia persistence

To investigate how the leading edge would behave when cells express different amounts of CRMP-1, we analyzed the behavior of the leading edge from kymographs generated from time-lapse imaging (Fig. 9 A). Kymographs showed that lamellipodia of control cells protruded forward persistently. The lamellipodia from CRMP-1–overexpressing cells also protruded forward, but they extended faster than those of the scramble cells. CRMP-1–depleted cells rarely formed protrusions (Fig. 7, B and C), and the wounded edge did not advance (Fig. 9 A, middle). However, a small percentage of CRMP-1–

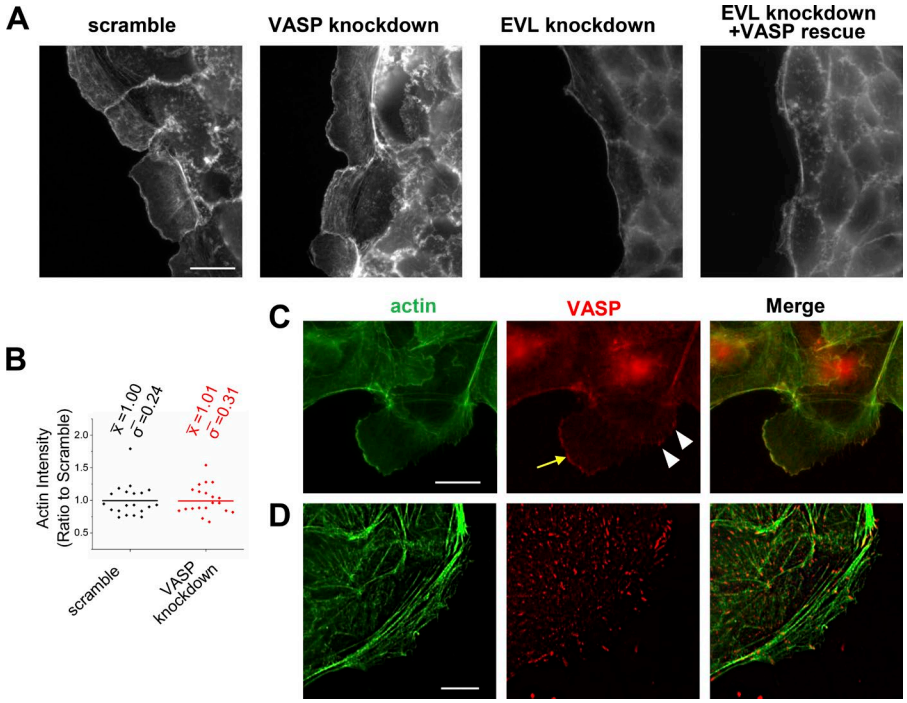

Figure 8. **VASP localizes to focal adhesions and lamellipodia in MDCK cells.** (A) Depletion of VASP did not affect lamellipodia formation. VASP did not rescue EVL-depleted cells' inability to form lamellipodia. (B) Quantification of A. Actin intensity at the leading edge of lamellipodia in scramble and VASP knockdown cells. Each dot indicates the result from one lamellipodium. (C and D) VASP localizes the leading edge of cells that make strong lamellipodia (yellow arrow) and focal adhesions (white arrowhead) in cells that make small protrusions. Focal adhesions are obvious in D while using mouse monoclonal antibody clone 43 (see Materials and methods). Bars, 10 µm.

depleted cells formed small protrusions. We analyzed the behavior of these small protrusions that managed to form in CRMP-1–depleted cells and found that they were unstable and retracted frequently (Fig. 9 B). Quantitative results confirmed that protrusions made by CRMP-1 knockdown cells showed the least persistence and greatest retraction frequency. Lamellipodia from CRMP-1–overexpressing cells and scramble controls had similar protrusion persistence, but the lamellipodia of CRMP-1–overexpressing cells advanced a greater distance of ∼4.7 µm/protrusion over a 5-min period compared with scrambles, at 1.3 and 1.8 µm/protrusion for the protrusions made in CRMP-1–depleted cells (Fig. 9 C).

CRMP-1 is important for cell–cell adhesion

The actin cytoskeleton helps support the integrity of epithelial sheets by bolstering adhesion systems such as E-cadherin–dependent adherens junctions, which are actin dependent. A prediction therefore is that a loss of CRMP-1 or any other factor necessary for assembling actin at cell–cell contacts will result in less cell–cell adhesion. This is clearly the case. Cells depleted of CRMP-1, Arp2/3, or EVL had holes in the monolayer that could be readily seen in light micrographs imaging for F-actin. An example of a hole in the monolayer in CRMP-depleted cells as detected with phalloidin staining is shown in Fig. 10 A. Holes also can be seen in cells depleted of components of the Arp2/3 complex or EVL (Figs. 2 A and 6 D). We compared the number of holes in sheets of control MDCK cells versus those depleted of the various factors. Holes were never seen in control MDCK cells, which is consistent with their physiological function. In contrast, cells depleted of factors necessary for the assembly of junctional or apical cortical actin had many holes. Expressing VASP in cells depleted of EVL did not rescue the integrity of the monolayer (Fig. 10 B).

To confirm that CRMP-1 knockdown indeed compromises cell–cell adhesion, we used hanging-drop adhesions assays to monitor cell clustering. We also used trituration to test the resistance of the cell aggregates to a shearing force. At the beginning of the hanging-drop experiment, both control cells and CRMP-1 knockdown cells were present as single cells or clusters of fewer than 10 cells (Fig. 10, C and D, 0 h). Before trituration, 30% of control cells were in large clusters of 50 cells or more after 2 h of aggregation in the hanging drop. This number increased to nearly 60% at 3 h. In contrast, the majority of CRMP-1–depleted cells remained as small clusters even at 3 h. After 4 h, 70% of the cells were in large clusters in CRMP-1–depleted conditions, whereas the control condition had already reached 98%. Therefore, CRMP-1–depleted cells aggregate at a slower rate than controls.

Control cells showed stronger resistance to trituration than CRMP-1–depleted cells. Control cells aggregated for 3 h showed the same clustering profile as CRMP-1 cells aggregated for 4 h. We therefore compared the ability of these two populations to resist trituration. After trituration, large clusters were all broken down to smaller sizes in CRMP-1–depleted cells, whereas ∼50% of the control cells remained in large clusters. Holes in the monolayer along with the cell adhesion assays show that CRMP-1 is important for cell–cell adhesion.

Discussion

CRMP-1 is one member of a family of five related factors that modulate the cytoskeleton to control such processes as growth cone motility, cell migration, neuronal and T cell polarity, and cancer cell metastasis (Wang and Strittmatter, 1996; Shih et al., 2003; Giraudon et al., 2013; Qiao et al., 2015; Xu et al., 2015). Previous results suggest that CRMPs perform these functions either by binding to tubulin dimers and promoting microtubule assembly (Gu and Ihara, 2000; Inagaki et al., 2001; Fukata et al., 2002) or by modulating actin filament bundling (Rosslenbroich et al., 2005; Yoneda et al., 2012; Khazaei et al., 2014; Norris et al., 2014; Yu-Kemp and Brieher, 2016). Our results demonstrate that CRMP-1 plays an important role in actin assembly. CRMP-1 was necessary for the assembly of actin filaments in the apical

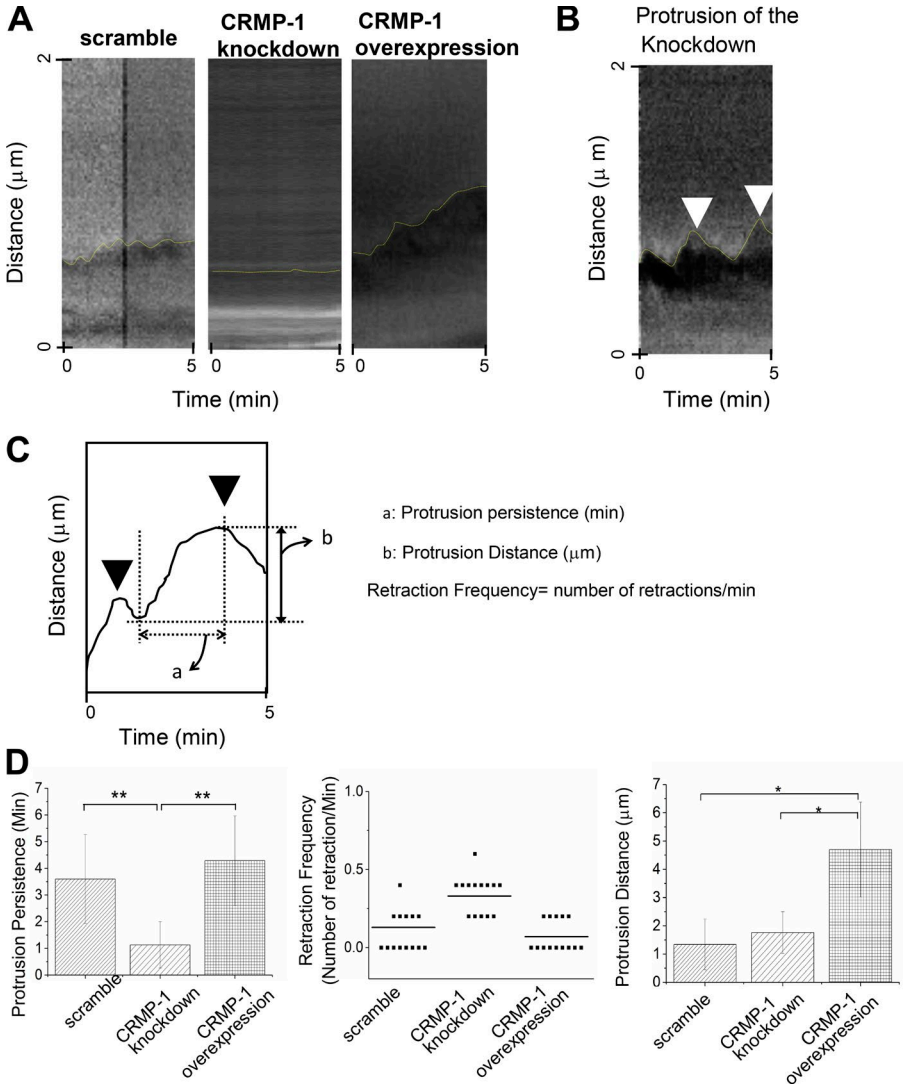

Figure 9. **CRMP-1 contributes to the persistence of the protruding edge in wounded monolayers.** (A) Representative kymographs of the protrusive edge. *x* axis represents time (minutes); *y* axis represents distance (micrometers). Note that the majority of cells depleted of CRMP-1 do not form protrusive structures. (B) Representative kymograph of a protrusion that did manage to form in CRMP-1–depleted cells. Triangle indicates the start of the retraction. The edge of the kymographs in A and B are highlighted with yellow dotted lines to help visualize the protrusion/retraction behavior of the leading edge. (C) Schematic representation of the parameters and the equation used for data analysis. (D) Quantification of A. Leading edges that do form in CRMP-1–depleted cells exhibit high retraction frequencies. CRMP-1–overexpressing cells protrude more persistently compared with control and CRMP knockdown cells. *, $P < 0.05$; **, $P < 0.01$ Graphs show the mean ± SD.

cortex and in lamellipodia. CRMP-1 might also contribute to the actin assembly at cell–cell adhesive contacts, which would help explain why perturbing CRMP-1 leads to a decrease in cell–cell adhesion. CRMP-1 is also important for the assembly of *Listeria* actin comet tails (Yu-Kemp and Brieher, 2016). CRMP-1 binds directly to EVL and stimulates EVL's intrinsic actin filament elongation activity. We therefore propose that a major function of CRMP-1 is to facilitate the assembly of actin networks by accelerating actin filament elongation rates. Defects in actin polymerization could easily account for the various phenotypes that result from perturbing CRMP function in other cell types. Physiological regulation of CRMP-dependent actin polymerization could also explain how CRMPs control neuronal growth advance in response to guidance cues such as Semaphorin 3A.

We found that CRMP-1 binds to EVL and promotes its ability to elongate actin filaments. EVL is related to VASP and Ena, and all three proteins are weakly processive actin filament elongation factors (Kühnel et al., 2004; Barzik et al., 2005; Applewhite et al., 2007; Ferron et al., 2007; Breitsprecher et al., 2008; Pasic et al., 2008; Hansen and Mullins, 2010; Winkelman et al., 2014). All three family members contain an EVH1 domain that is separated from an EVH2 domain by a proline-rich segment. The EVH1 domain targets the protein to different locations within the cell (Bear and Gertler, 2009). The EVH2 domain binds to F-actin and G-actin and is responsible for accelerating barbed-end growth (Bachmann et al., 1999; Ferron et al., 2007). Current models of elongation propose that actin monomers are transferred from Ena/VASP to the growing barbed end to which Ena/VASP is attached. CRMP-1 binds to the EVH2 domain of EVL, and CRMP-1 also binds to F-actin. Therefore, CRMP-1 could promote EVL-dependent actin elongation by increasing either the rate at which actin monomers are transferred from the EVH2 G-actin binding site to the barbed end or the affinity of EVH2 for F-actin. Our results favor the former mechanism, because we did not detect a change in the concentration of EVL required to reach the half-maximal rate in elongation with or without CRMP. Although Ena/VASP/EVL interact with many different proteins, profilin and lamellipodin are the only other binding partners known to modulate elongation activity (Hansen and Mullins, 2010, 2015). Profilin binds to the proline-rich domain (Reinhard et al., 1995; Kang et al., 1997; Ferron et al., 2007), lamellipodin binds to EVH1, and CRMP-1 binds to EVH2 (Krause et al., 2004; Hansen and Mullins, 2015). EVH2 can be phosphorylated by protein kinase A and protein kinase G. These phosphorylations are known to alter VASP binding to F-actin (Benz et al., 2009). Phosphorylation of EVH2 might also control its ability to bind CRMP-1, to provide cells with an additional control point to modulate actin polymerization.

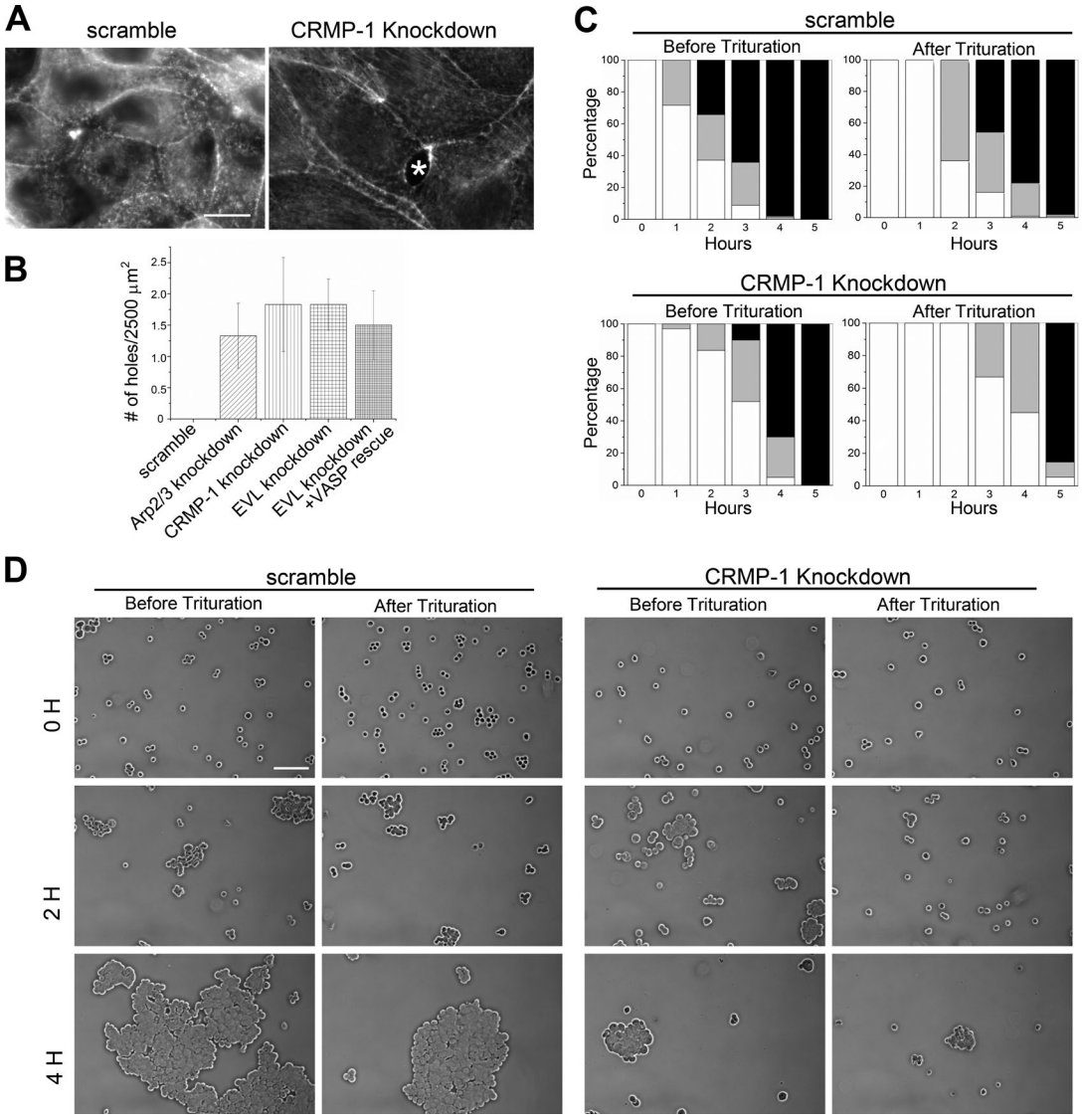

Figure 10. **CRMP-1 knockdown cells show weaker cell–cell adhesion.** (A) Phalloidin staining of confluent monolayers of scramble and CRMP-1 knockdown cells. White star indicates a hole in the monolayer. Bar, 10 µm. (B) Quantifications showing that cells depleted of Arp2/3, CRMP-1, or EVL contain holes in the monolayer. For each condition (scramble, Arp2/3 knockdown, CRMP-1 knockdown, and EVL knockdown), the number of holes was quantified from three individual sets of data. Graph shows means ± SD. (C and D) Hanging-drop experiments showing that CRMP-1–depleted cells have decreased cell–cell adhesion. (C) Quantification. The stacked column represents the percentage of cells in clusters as 0–10 cells (white), 11–50 cells (gray), or >50 cells (black). (D) Representative images of cell clusters from the hanging-drop experiments. Images were collected at 0, 2, and 4 h, before and after trituration. Bar, 100 µm.

CRMP-1 and EVL proved to be just as important as Arp2/3 and WAVE2 for assembly of the actin cortex, actin at adherens junctions, and lamellipodia in MDCK cells. This could mean that actin filament elongation reactions are especially important in MDCK cells. Such a situation could arise if the cells contained very high concentrations of capping protein, which binds to barbed ends and terminates further growth (Edwards et al., 2014). Ena/VASP/EVL can antagonize capping protein, but the effect is weak (Bear et al., 2002; Barzik et al., 2005; Breitsprecher et al., 2008; Pasic et al., 2008; Hansen and Mullins, 2010). Not only might CRMP-1 accelerate actin filament elongation rates, it might also help EVL shield barbed ends from capping protein. Alternatively, CRMP-1 and EVL might contribute to the assembly of Arp2/3-WAVE–dependent actin assembly in other ways. For example, VASP binds to WAVE (Havrylenko et al., 2015) and CRMP-1 binds to the WAVE-associated protein Sra1 (Kawano et al., 2005), which is important for WAVE- and Arp2/3-dependent lamellipodia formation (Kunda et al., 2003). Therefore, in addition to elongating filaments, CRMP and EVL might also contribute to Arp2/3 activation in lamellipodia.

Ena, VASP, and EVL are homologous, with shared biochemical activities. Deleting all three genes in mice produces a more severe phenotype than deleting any individual gene or pair of genes, underscoring their functional redundancy (Kwiatkowski et al., 2007). Nevertheless, VASP was unable to substitute for EVL in MDCK cells. Although EVL produced the exact same actin networks as CRMP-1, WAVE2, and Arp2/3, VASP assembled more actin stress fibers on the basal surface of the cell, which has been seen before. Our data also revealed that EVL is important for lamellipodia formation in MDCK cells; yet VASP is not. An earlier study in fibroblasts showed that perturbing Ena/VASP did not affect the formation of lamellipodia

yet altered the persistency of the protrusion (Bear et al., 2002). Although Ena, VASP, and EVL have similar biochemical properties in vitro, they might contribute to the assembly of different actin networks in different types of cells. Other compensatory mechanisms might be masking interesting differences between the family members in the whole organism (Withee et al., 2004).

Cells depleted of CRMP-1, EVL, WAVE2, or components of the Arp2/3 complex spread extensively, producing an enormous apical membrane (at the expense of lateral membrane), resulting in very thin cells. The phenotype eventually corrects itself, at least to some extent, as the cells pack more as the monolayer ages. This phenotype has been seen before. Inhibition of the pointed actin capping protein tropomodulin, ankyrin, or p120 catenin produces thin cells with increased apical surface per cell and reduced lateral membrane (Kizhatil and Bennett, 2004; Kizhatil et al., 2007; Weber et al., 2007; Bulgakova and Brown, 2016; Yu et al., 2016). Therefore, ankyrin-, actin-, and cadherin-mediated cell–cell adhesions all determine whether cells preferentially spread on the extracellular matrix or on each other to expand the lateral membrane. The increase in cell spreading in the plane of the substrate also correlated with a possible doubling in cell volume and nuclear size.

Epithelial cells form extensive cell–cell adhesive junctions that are essential for epithelial tissue to create a barrier separating two distinct environments. E-cadherin is the major cell–cell adhesion molecule expressed in epithelial cells, and its activity is actin dependent. We have shown that CRMP-1, EVL, WAVE2, and Arp2/3 are all critical for the formation of the apical actin cortex and assembly of the actin cytoskeleton at cell–cell contacts. As a consequence, perturbing any of these proteins compromises cell–cell adhesion, resulting in holes in the epithelial sheet, which is catastrophic for epithelial function. Research on cadherin–actin interactions has thus far focused on how α-catenin links cadherins to actin filaments that are under myosin II–dependent tension (le Duc et al., 2010; Yonemura et al., 2010; Buckley et al., 2014; Nelson and Weis, 2016). Our results here show that actin polymerization is at least as important for cell–cell adhesion and the structural integrity of epithelial sheets as mechanically stable linkages that connect cadherins to contractile actin networks. When Arp2/3-, EVL-, or CRMP-1–mediated actin filament dynamics fail, the monolayer becomes perforated with holes that will have a harder time healing, because these same factors are critical for lamellipodia formation that could quickly seal the wound.

Materials and methods

Plasmids and protein purification

For recombinant protein expression, human CRMP-1 or human EVL (full length, EVH1 domain, and EVH2 domain) was cloned into pET30a. Human CRMP-1 or human EVL was also cloned into pMALc4x for testing protein interactions. Truncations of mouse WAVE2 (VCA region alone or deletion of 272 aa from the N terminus [δ273]) were cloned into the pGEX 5X-1. VVCA region of WAVE was provided by the D. Kovar laboratory (University of Chicago, Chicago, IL; Skau et al., 2011). Human VASP was cloned into pEX-N-His (OriGene). The EVH2 domain of human Mena was provided by J. Faix (Hannover Medical School, Hannover, Germany; Breitsprecher et al., 2011). Rosetta *Escherichia coli* cells (EMD Millipore) were used for expressing recombinant proteins. All the recombinant proteins were induced when bacterial OD reached 0.5. All the recombinant proteins were induced with 0.2 mM IPTG at RT for 4 h. The purification of each protein was done according to manufacturer's instructions for His-tagged (QIAGEN) and GST-tagged and MBP-tagged (GE Healthcare) proteins.

Cells and cell transfection

Madin-Darby canine kidney II cells (MDCK II) were used for the experiments. The cells were cultured at 37°C under 5% CO_2 in DMEM with 5% FBS. Knockdown cells were generated by calcium phosphate precipitation with shRNAs when the cells reached 50% confluence. 24 h after transfection, cells were trypsinized and plated into puromycin or G418 for 24 h. Selection drugs were removed after 24 h. A heterogeneous cell population was collected and used for the experiments within 1 wk after transfection. Western blotting was used to validate knockdown efficiency. For Western blotting, we used a detergent-compatible Bradford assay (Bio-Rad Laboratories) to verify that the same amount of sample from different conditions was provided for each lane. The primary antibodies used for each Western blotting are homemade rabbit polyclonal antibodies (for CRMP-1 or EVL); for Arp3 or p34, p34 antibody (07-227; EMD Millipore) or Arp3 antibody (sc-10130; Santa Cruz Biotechnology, Inc.); VASP antibody (3112; Cell Signaling Technology); and WAVE2 antibody (sc-33548; Cell Signaling Technology).

For shRNA-expressing plasmids, hybridized oligonucleotides were cloned into pLKO.1. The following target sequences were used: Scramble, plasmid 1864 (Addgene); CRMP-1 sh1, 5′-ACCTGGAAG ATGGACTTATAA-3′; CRMP-1 sh2, 5′-CCAAGTCTACATGGCATA TAA-3′; CRMP-1 sh3, 5′-GATGGATGAGCTAGGAATAAA-3′; p34 shRNA1, 5′-TACGGGAGTTTCTTGGTAAAT-3′; p34 shRNA2, 5′-TACAATGTCTCTTTGCTATAT-3′; p34 shRNA3, 5′-GCCTCTGTC TTTGAGAAATAT-3′; APR2 shRNA1, 5′-GTAGATGCCAGACTG AAATTA-3′; ARP3 shRNA2, 5′-AGAAATTGGACCTAGCATTTG-3′; ARP3 shRNA3, 5′-GTCGTCACAATCCAGTGTTTG-3′; EVL shRNA1, 5′-CAGCAGGTTGTGATCAATTAT-3′; EVL shRNA2, 5′-AGGAGGCCTCATGGAAGAAAT-3′; WAVE2 shRNA1, 5′-TGG GCAGCCTGAGTAAATATG-3′; and WAVE2 shRNA2, 5′-TCC AAATCGAGGGAATGTAAA-3′. VASP shRNA was purchased from OriGene: 5′-ATGAGTGAGACGGTTATCTGCTCCAGCTG-3′. CRMP-1 rescue was done with human CRMP-1 cloned into pLenti-III-HA (ABM Inc.); VASP rescue was done with a vector purchased from OriGene (mr205851).

Actin polymerization assays

Pyrene actin was prepared as described (Bryan and Coluccio, 1985). Actin polymerization was monitored by the increase in fluorescence of pyrenyl-actin with excitation at 365 nm and emission at 410 nm. The reaction contains 2.5 µM actin (25% pyrene-labeled), with various proteins added as indicated in the figures. The reaction was carried in buffer A (1 mM EGTA, 50 mM KCl, 1 mM $MgCl_2$, and 10 mM imidazole, pH 7.0, with 2 mM ATP). To address the change of polymerization rate in Fig. 2, we calculated the slope of the curves 3 min before and after CRMP-1 was added.

Protein interactions

The affinity of CRMP-1 for EVL was determined using the approach described by Pollard (2010). We used recombinant MBP-tagged proteins or His-tagged proteins to test protein interactions. MBP-CRMP-1 or MBP-EVL was immobilized onto amylose beads (New England Biolabs, Inc.). To determine the amount of MBP-tagged protein bound to the beads, Bradford assay (Bio-Rad Laboratories) was used to measure the amount of protein left in the supernatant. The amylose beads were blocked with 0.5% casein by rocking at 4°C for 1 h before use. To test CRMP-1 and EVL (full length) interaction, a constant amount of His-

CRMP-1 was incubated with varying amounts of MBP-EVL beads. Three repeats of experiments were done to calculate the binding curve of CRMP-1 and EVL (full length). To test the CRMP-1 binding domain on EVL, we incubated MBP-CRMP-1 beads with solution containing EVH1 or EVH2 fragments. Each condition contained 200-µl solutions. After 1 h of incubation at 4°C, the beads were pelleted using centrifugation. The supernatant was collected and loaded into SDS-PAGE. The amount of protein remaining in the supernatant was verified by either Coomassie staining or Western blotting.

Time-lapse single-filament assay

Filaments were polymerized by incubating 1 µM Alexa Fluor 647–labeled actin (15% labeled) or rhodamine-labeled actin (20% labeled) in buffer A in the presence of antibleaching reagents (15 mM glucose, 20 µg/ml catalase, 100 µg/ml glucose oxidase, and 1 mM Trolox) for 1 min at RT. The reaction had a total volume of 25 ml. For control conditions (actin alone and "+ 60 nM CRMP-1"), the reactions were started with actin alone in the test tube without EVL. After 1-min incubation, buffer (actin alone) or 60 nM CRMP-1 was added to the test tube. For other conditions, the actin was polymerized with EVL for 1 min and different concentrations of CRMP-1 were later added: 25 nM EVL (no CRMP-1 was added) or EVL + X nM CRMP-1, where X is the amount of CRMP-1 in nanomoles. To visualize filament growth, 2 µl of the reaction was placed on to the coverslip and immediately imaged under a fluorescence microscope. The coverslip was precoated with 1 µM α-actinin-4 to capture filaments. The images were collected every 3 s for 3 min with 2 × 2 binning under a 63× objective lens (NA 1.4) attached to a 1,000 × 1,000 CCD camera (ORCA-ER; Hamamatsu Photonics) on an AxioImager1 (ZEISS) with the Colibri illumination system or to Axiocam 503 mono on an AxioImager2 under acquisition software (ZEISS).

Immunofluorescence and live-cell imaging of MDCK II

Immunostaining of different proteins was done with antibodies listed in Cells and cell transfection. Cells were extracted with Triton X-100 before formaldehyde fixation. Extraction buffer contains 50 mM NaCl, 3 mM $MgCl_2$, 10 mM Hepes, pH 6.8, and 0.5% Triton X-100. Primary antibodies were diluted 1:200, followed by a secondary antibody conjugated with fluorophore (Thermo Fisher Scientific) at 1:200 dilution in PBS for 1 h. Immunostaining of VASP was performed with rabbit polyclonal antibody from Cell Signaling Technology (3112; Fig. 8 C) or mouse monoclonal antibody from BD (clone 43; Fig. 8 D). E-Cadherin immunostaining was done with rr1 antibody (Developmental Studies Hybridoma Bank), which is specific for canine E-cadherin (Gumbiner and Simons, 1986). Actin staining was done using phalloidin according to the manufacturer's instruction (Alexa Fluor 647 phalloidin from Thermo Fisher Scientific or FITC-phalloidin from American Peptide Company).

Fluorescence images were collected using two different microscopes: Applied Precision personal DeltaVision deconvolution microscope system (GE Healthcare) with a 60× (1.4-NA) objective lens and a CoolSNAP HQ2 CCD camera (Figs. 1, 2, 3, 6 [except B and F], 7 B, 8 D, and 9 A) or with a 63× objective on a ZEISS AxioImager (Figs. 5, 6 [B and F], 7 [A and D], 8 [A and C], and 10). For detecting lamellipodia formation in response to wounding, a sharpened needle was used to wound a confluent MDCK II monolayer grown on collagen-coated coverslips. A 1-h serum starvation step was performed before wounding if needed. The monolayers were then allowed to recover in MEM with 5% FBS for 1 h before immunostaining. Cell protrusive activity under wound-healing conditions was imaged at 24.5°C. Phase-contrast images were acquired every 5 s for a total of 5 min using a 40× phase-contrast objective lens (NA 0.7) with the ORCA-ER camera.

Adhesion and trituration assay

This assay was performed as described by the Nelson group with some modifications (Ehrlich et al., 2002). In brief, cells were allowed to grow in a 10-cm dish for 2 d. Cells were trypsinized, centrifuged, and resuspended in the media at 1.2×10^6 cells/ml. 20-µl drops of cell suspension were pipetted on the inside surface of 6-cm culture dish lids. At the bottom of the dish, 5 ml medium was added to prevent evaporation. At each time point, two individual drops were used and quantified. Each drop had 5 µl suspension spread directly on the glass slide, as the sample before trituration. Another 5 µl suspension was taken out from each drop and triturated 10 times with a 20-ml pipet before being put on a glass slide. At least three random fields from each drop were photographed under a 20× objective on the AxioImager. The number of cells and size of clusters were determined. Note that same amount of cells were quantified in different conditions.

Data analysis

Data analysis of the results was performed with Fiji software (Schindelin et al., 2012). To quantify and compare the amount of actin, we analyzed the images taken under the DeltaVision microscope system. To quantify the amount of actin around cell–cell borders, we manually outlined the two cell boundaries and measured the fluorescence intensity per pixel. For quantifying the amount of cortical actin, three 1 × 1-µm boxes were drawn inside one cell. The actin intensity was collected and averaged from these three datasets. Each dot shown in the figures is the result of an individual measurement. To quantify the percentage of wounded edge covered by lamellipodia, we divided the number of protrusions by the total number of cells at the wounded edge. Each quantification was done by analyzing the cells in a 50 × 50-µm square; 15 sets of squares were counted for each condition. To estimate the cell volume difference between scramble and CRMP-1 knockdown cells, images from hanging-drop experiments were used to measure the radius of individual cells. To estimate nuclear size change, we measured the radius of the nucleus (using DAPI signal) in the middle of the cell in a monolayer. To analyze single-filament results, 30 filaments of each condition in each set were counted; the results were analyzed from three repeats. Each dot shown in Fig. 5 B represents a filament. To quantify whether the number of filaments was increased by time in each condition, the number of filaments in a 15 × 15-µm box was analyzed. N* in Fig. 5 A is the mean number of filaments after this quantification. For live-cell imaging, the tracking plug-in of Fiji was used to track the movement of the leading edge. The middle of the leading edge was followed to track the movement and generate the kymograph.

Online supplemental material

Fig. S1 shows CRMP-1 and actin staining in control and CRMP-1–depleted cells. Fig. S2 shows Western blots of target proteins in control cells versus shRNA knockdown cells. Fig. S3 shows estimates of cell volume in control and CRMP-1–depleted cells. Fig. S4 shows a Western blot of CRMP-1 in liver membranes.

Acknowledgments

We are grateful to Dr. David Kovar for providing VVCA construct and Dr. Jan Faix for providing the Mena-EVH2 construct. We thank Guillaume Romet-Lemonne (Institut Jacques Monod) and Vivian Tang (University of Illinois) for suggesting that polymerization of single filaments could be imaged using widefield microscopy and Yuou Wang (University of Illinois) for working out the initial conditions for such imaging. We thank Dr. Jon Henry (University of Illinois) for use of his microscope.

This work is funded by National Institutes of Health grant R01-GM106106 and American Heart Association Scientist Development Grant 0930282G, both to W.M. Brieher.

The authors declare no competing financial interests.

Author contributions: H.-C. Yu-Kemp and W.M. Brieher conceived and performed experiments and wrote the paper. J.P. Kemp Jr. helped adjust experimental conditions for transfection and staining, performed VASP staining in wounded monolayers, purified recombinant CRMP-1, and purified E-cadherin antibodies (RR1) from hybridoma.

Submitted: 17 June 2016
Revised: 4 January 2017
Accepted: 12 May 2017

References

Abu Taha, A., M. Taha, J. Seebach, and H.J. Schnittler. 2014. ARP2/3-mediated junction-associated lamellipodia control VE-cadherin-based cell junction dynamics and maintain monolayer integrity. *Mol. Biol. Cell.* 25:245–256. http://dx.doi.org/10.1091/mbc.E13-07-0404

Applewhite, D.A., M. Barzik, S. Kojima, T.M. Svitkina, F.B. Gertler, and G.G. Borisy. 2007. Ena/VASP proteins have an anti-capping independent function in filopodia formation. *Mol. Biol. Cell.* 18:2579–2591. http://dx.doi.org/10.1091/mbc.E06-11-0990

Arimura, N., N. Inagaki, K. Chihara, C. Ménager, N. Nakamura, M. Amano, A. Iwamatsu, Y. Goshima, and K. Kaibuchi. 2000. Phosphorylation of collapsin response mediator protein-2 by Rho-kinase. Evidence for two separate signaling pathways for growth cone collapse. *J. Biol. Chem.* 275:23973–23980. http://dx.doi.org/10.1074/jbc.M001032200

Bachmann, C., L. Fischer, U. Walter, and M. Reinhard. 1999. The EVH2 domain of the vasodilator-stimulated phosphoprotein mediates tetramerization, F-actin binding, and actin bundle formation. *J. Biol. Chem.* 274:23549–23557. http://dx.doi.org/10.1074/jbc.274.33.23549

Barzik, M., T.I. Kotova, H.N. Higgs, L. Hazelwood, D. Hanein, F.B. Gertler, and D.A. Schafer. 2005. Ena/VASP proteins enhance actin polymerization in the presence of barbed end capping proteins. *J. Biol. Chem.* 280:28653–28662. http://dx.doi.org/10.1074/jbc.M503957200

Bear, J.E., and F.B. Gertler. 2009. Ena/VASP: Towards resolving a pointed controversy at the barbed end. *J. Cell Sci.* 122:1947–1953. http://dx.doi.org/10.1242/jcs.038125

Bear, J.E., T.M. Svitkina, M. Krause, D.A. Schafer, J.J. Loureiro, G.A. Strasser, I.V. Maly, O.Y. Chaga, J.A. Cooper, G.G. Borisy, and F.B. Gertler. 2002. Antagonism between Ena/VASP proteins and actin filament capping regulates fibroblast motility. *Cell.* 109:509–521. http://dx.doi.org/10.1016/S0092-8674(02)00731-6

Benz, P.M., C. Blume, S. Seifert, S. Wilhelm, J. Waschke, K. Schuh, F. Gertler, T. Münzel, and T. Renné. 2009. Differential VASP phosphorylation controls remodeling of the actin cytoskeleton. *J. Cell Sci.* 122:3954–3965. http://dx.doi.org/10.1242/jcs.044537

Breitsprecher, D., A.K. Kiesewetter, J. Linkner, C. Urbanke, G.P. Resch, J.V. Small, and J. Faix. 2008. Clustering of VASP actively drives processive, WH2 domain-mediated actin filament elongation. *EMBO J.* 27:2943–2954. http://dx.doi.org/10.1038/emboj.2008.211

Breitsprecher, D., A.K. Kiesewetter, J. Linkner, M. Vinzenz, T.E. Stradal, J.V. Small, U. Curth, R.B. Dickinson, and J. Faix. 2011. Molecular mechanism of Ena/VASP-mediated actin-filament elongation. *EMBO J.* 30:456–467. http://dx.doi.org/10.1038/emboj.2010.348

Brieher, W.M., M. Coughlin, and T.J. Mitchison. 2004. Fascin-mediated propulsion of *Listeria monocytogenes* independent of frequent nucleation by the Arp2/3 complex. *J. Cell Biol.* 165:233–242. http://dx.doi.org/10.1083/jcb.200311040

Brittain, J.M., A.D. Piekarz, Y. Wang, T. Kondo, T.R. Cummins, and R. Khanna. 2009. An atypical role for collapsin response mediator protein 2 (CRMP-2) in neurotransmitter release via interaction with presynaptic voltage-gated calcium channels. *J. Biol. Chem.* 284:31375–31390. http://dx.doi.org/10.1074/jbc.M109.009951

Bryan, J., and L.M. Coluccio. 1985. Kinetic analysis of F-actin depolymerization in the presence of platelet gelsolin and gelsolin-actin complexes. *J. Cell Biol.* 101:1236–1244. http://dx.doi.org/10.1083/jcb.101.4.1236

Buckley, C.D., J. Tan, K.L. Anderson, D. Hanein, N. Volkmann, W.I. Weis, W.J. Nelson, and A.R. Dunn. 2014. Cell adhesion. The minimal cadherin-catenin complex binds to actin filaments under force. *Science.* 346:1254211. http://dx.doi.org/10.1126/science.1254211

Bulgakova, N.A., and N.H. Brown. 2016. *Drosophila* p120-catenin is crucial for endocytosis of the dynamic E-cadherin-Bazooka complex. *J. Cell Sci.* 129:477–482. http://dx.doi.org/10.1242/jcs.177527

Derivery, E., C. Sousa, J.J. Gautier, B. Lombard, D. Loew, and A. Gautreau. 2009. The Arp2/3 activator WASH controls the fission of endosomes through a large multiprotein complex. *Dev. Cell.* 17:712–723. http://dx.doi.org/10.1016/j.devcel.2009.09.010

Duncan, M.C., M.J. Cope, B.L. Goode, B. Wendland, and D.G. Drubin. 2001. Yeast Eps15-like endocytic protein, Pan1p, activates the Arp2/3 complex. *Nat. Cell Biol.* 3:687–690. http://dx.doi.org/10.1038/35083087

Edwards, M., A. Zwolak, D.A. Schafer, D. Sept, R. Dominguez, and J.A. Cooper. 2014. Capping protein regulators fine-tune actin assembly dynamics. *Nat. Rev. Mol. Cell Biol.* 15:677–689. http://dx.doi.org/10.1038/nrm3869

Egile, C., T.P. Loisel, V. Laurent, R. Li, D. Pantaloni, P.J. Sansonetti, and M.F. Carlier. 1999. Activation of the CDC42 effector N-WASP by the *Shigella flexneri* IcsA protein promotes actin nucleation by Arp2/3 complex and bacterial actin-based motility. *J. Cell Biol.* 146:1319–1332. http://dx.doi.org/10.1083/jcb.146.6.1319

Ehrlich, J.S., M.D. Hansen, and W.J. Nelson. 2002. Spatio-temporal regulation of Rac1 localization and lamellipodia dynamics during epithelial cell-cell adhesion. *Dev. Cell.* 3:259–270. http://dx.doi.org/10.1016/S1534-5807(02)00216-2

Enyedi, B., and P. Niethammer. 2015. Mechanisms of epithelial wound detection. *Trends Cell Biol.* 25:398–407. http://dx.doi.org/10.1016/j.tcb.2015.02.007

Ferron, F., G. Rebowski, S.H. Lee, and R. Dominguez. 2007. Structural basis for the recruitment of profilin-actin complexes during filament elongation by Ena/VASP. *EMBO J.* 26:4597–4606. http://dx.doi.org/10.1038/sj.emboj.7601874

Frischknecht, F., V. Moreau, S. Röttger, S. Gonfloni, I. Reckmann, G. Superti-Furga, and M. Way. 1999. Actin-based motility of vaccinia virus mimics receptor tyrosine kinase signalling. *Nature.* 401:926–929. http://dx.doi.org/10.1038/44860

Fukata, Y., T.J. Itoh, T. Kimura, C. Ménager, T. Nishimura, T. Shiromizu, H. Watanabe, N. Inagaki, A. Iwamatsu, H. Hotani, and K. Kaibuchi. 2002. CRMP-2 binds to tubulin heterodimers to promote microtubule assembly. *Nat. Cell Biol.* 4:583–591.

Furman, C., A.L. Sieminski, A.V. Kwiatkowski, D.A. Rubinson, E. Vasile, R.T. Bronson, R. Fässler, and F.B. Gertler. 2007. Ena/VASP is required for endothelial barrier function in vivo. *J. Cell Biol.* 179:761–775. http://dx.doi.org/10.1083/jcb.200705002

Giraudon, P., A. Nicolle, S. Cavagna, C. Benetollo, R. Marignier, and M. Varrin-Doyer. 2013. Insight into the role of CRMP2 (collapsin response mediator protein 2) in T lymphocyte migration: The particular context of virus infection. *Cell Adhes. Migr.* 7:38–43. http://dx.doi.org/10.4161/cam.22385

Goley, E.D., and M.D. Welch. 2006. The ARP2/3 complex: an actin nucleator comes of age. *Nat. Rev. Mol. Cell Biol.* 7:713–726. http://dx.doi.org/10.1038/nrm2026

Goshima, Y., F. Nakamura, P. Strittmatter, and S.M. Strittmatter. 1995. Collapsin-induced growth cone collapse mediated by an intracellular protein related to UNC-33. *Nature.* 376:509–514. http://dx.doi.org/10.1038/376509a0

Gu, Y., and Y. Ihara. 2000. Evidence that collapsin response mediator protein-2 is involved in the dynamics of microtubules. *J. Biol. Chem.* 275:17917–17920. http://dx.doi.org/10.1074/jbc.C000179200

Gumbiner, B., and K. Simons. 1986. A functional assay for proteins involved in establishing an epithelial occluding barrier: Identification of a uvomorulin-like polypeptide. *J. Cell Biol.* 102:457–468. http://dx.doi.org/10.1083/jcb.102.2.457

Haffner, C., T. Jarchau, M. Reinhard, J. Hoppe, S.M. Lohmann, and U. Walter. 1995. Molecular cloning, structural analysis and functional expression of the proline-rich focal adhesion and microfilament-associated protein VASP. *EMBO J.* 14:19–27.

Hansen, S.D., and R.D. Mullins. 2010. VASP is a processive actin polymerase that requires monomeric actin for barbed end association. *J. Cell Biol.* 191:571–584. http://dx.doi.org/10.1083/jcb.201003014

Hansen, S.D., and R.D. Mullins. 2015. Lamellipodin promotes actin assembly by clustering Ena/VASP proteins and tethering them to actin filaments. *eLife.* 4:e06585. http://dx.doi.org/10.7554/eLife.06585

Havrylenko, S., P. Noguera, M. Abou-Ghali, J. Manzi, F. Faqir, A. Lamora, C. Guérin, L. Blanchoin, and J. Plastino. 2015. WAVE binds Ena/VASP for enhanced Arp2/3 complex-based actin assembly. *Mol. Biol. Cell.* 26:55–65. http://dx.doi.org/10.1091/mbc.E14-07-1200

Inagaki, N., K. Chihara, N. Arimura, C. Ménager, Y. Kawano, N. Matsuo, T. Nishimura, M. Amano, and K. Kaibuchi. 2001. CRMP-2 induces axons in cultured hippocampal neurons. *Nat. Neurosci.* 4:781–782. http://dx.doi.org/10.1038/90476

Jeng, R.L., E.D. Goley, J.A. D'Alessio, O.Y. Chaga, T.M. Svitkina, G.G. Borisy, R.A. Heinzen, and M.D. Welch. 2004. A Rickettsia WASP-like protein activates the Arp2/3 complex and mediates actin-based motility. *Cell. Microbiol.* 6:761–769. http://dx.doi.org/10.1111/j.1462-5822.2004.00402.x

Kang, F., R.O. Laine, M.R. Bubb, F.S. Southwick, and D.L. Purich. 1997. Profilin interacts with the Gly-Pro-Pro-Pro-Pro-Pro sequences of vasodilator-stimulated phosphoprotein (VASP): Implications for actin-based *Listeria* motility. *Biochemistry.* 36:8384–8392. http://dx.doi.org/10.1021/bi970065n

Kawano, Y., T. Yoshimura, D. Tsuboi, S. Kawabata, T. Kaneko-Kawano, H. Shirataki, T. Takenawa, and K. Kaibuchi. 2005. CRMP-2 is involved in kinesin-1-dependent transport of the Sra-1/WAVE1 complex and axon formation. *Mol. Cell. Biol.* 25:9920–9935. http://dx.doi.org/10.1128/MCB.25.22.9920-9935.2005

Khazaei, M.R., M.P. Girouard, R. Alchini, S. Ong Tone, T. Shimada, S. Bechstedt, M. Cowan, D. Guillet, P.W. Wiseman, G. Brouhard, et al. 2014. Collapsin response mediator protein 4 regulates growth cone dynamics through the actin and microtubule cytoskeleton. *J. Biol. Chem.* 289:30133–30143. http://dx.doi.org/10.1074/jbc.M114.570440

Kizhatil, K., and V. Bennett. 2004. Lateral membrane biogenesis in human bronchial epithelial cells requires 190-kDa ankyrin-G. *J. Biol. Chem.* 279:16706–16714. http://dx.doi.org/10.1074/jbc.M314296200

Kizhatil, K., W. Yoon, P.J. Mohler, L.H. Davis, J.A. Hoffman, and V. Bennett. 2007. Ankyrin-G and β2-spectrin collaborate in biogenesis of lateral membrane of human bronchial epithelial cells. *J. Biol. Chem.* 282:2029–2037. http://dx.doi.org/10.1074/jbc.M608921200

Krause, M., J.D. Leslie, M. Stewart, E.M. Lafuente, F. Valderrama, R. Jagannathan, G.A. Strasser, D.A. Rubinson, H. Liu, M. Way, et al. 2004. Lamellipodin, an Ena/VASP ligand, is implicated in the regulation of lamellipodial dynamics. *Dev. Cell.* 7:571–583. http://dx.doi.org/10.1016/j.devcel.2004.07.024

Kühnel, K., T. Jarchau, E. Wolf, I. Schlichting, U. Walter, A. Wittinghofer, and S.V. Strelkov. 2004. The VASP tetramerization domain is a right-handed coiled coil based on a 15-residue repeat. *Proc. Natl. Acad. Sci. USA.* 101:17027–17032. http://dx.doi.org/10.1073/pnas.0403069101

Kunda, P., G. Craig, V. Dominguez, and B. Baum. 2003. Abi, Sra1, and Kette control the stability and localization of SCAR/WAVE to regulate the formation of actin-based protrusions. *Curr. Biol.* 13:1867–1875. http://dx.doi.org/10.1016/j.cub.2003.10.005

Kwiatkowski, A.V., D.A. Rubinson, E.W. Dent, J. Edward van Veen, J.D. Leslie, J. Zhang, L.M. Mebane, U. Philippar, E.M. Pinheiro, A.A. Burds, et al. 2007. Ena/VASP is required for neuritogenesis in the developing cortex. *Neuron.* 56:441–455. http://dx.doi.org/10.1016/j.neuron.2007.09.008

le Duc, Q., Q. Shi, I. Blonk, A. Sonnenberg, N. Wang, D. Leckband, and J. de Rooij. 2010. Vinculin potentiates E-cadherin mechanosensing and is recruited to actin-anchored sites within adherens junctions in a myosin II-dependent manner. *J. Cell Biol.* 189:1107–1115. http://dx.doi.org/10.1083/jcb.201001149

Li, W., R.K. Herman, and J.E. Shaw. 1992. Analysis of the *Caenorhabditis elegans* axonal guidance and outgrowth gene unc-33. *Genetics.* 132:675–689.

Lin, P.C., P.M. Chan, C. Hall, and E. Manser. 2011. Collapsin response mediator proteins (CRMPs) are a new class of microtubule-associated protein (MAP) that selectively interacts with assembled microtubules via a taxol-sensitive binding interaction. *J. Biol. Chem.* 286:41466–41478. http://dx.doi.org/10.1074/jbc.M111.283580

Loisel, T.P., R. Boujemaa, D. Pantaloni, and M.F. Carlier. 1999. Reconstitution of actin-based motility of *Listeria* and *Shigella* using pure proteins. *Nature.* 401:613–616. http://dx.doi.org/10.1038/44183

Machesky, L.M., R.D. Mullins, H.N. Higgs, D.A. Kaiser, L. Blanchoin, R.C. May, M.E. Hall, and T.D. Pollard. 1999. Scar, a WASp-related protein, activates nucleation of actin filaments by the Arp2/3 complex. *Proc. Natl. Acad. Sci. USA*. 96:3739–3744. http://dx.doi.org/10.1073/pnas.96.7.3739

Maniar, T.A., M. Kaplan, G.J. Wang, K. Shen, L. Wei, J.E. Shaw, S.P. Koushika, and C.I. Bargmann. 2011. UNC-33 (CRMP) and ankyrin organize microtubules and localize kinesin to polarize axon-dendrite sorting. *Nat. Neurosci.* 15:48–56. http://dx.doi.org/10.1038/nn.2970

Marchiando, A.M., W.V. Graham, and J.R. Turner. 2010. Epithelial barriers in homeostasis and disease. *Annu. Rev. Pathol.* 5:119–144. http://dx.doi.org/10.1146/annurev.pathol.4.110807.092135

Martins-de-Souza, D., J.S. Cassoli, J.M. Nascimento, K. Hensley, P.C. Guest, A.M. Pinzon-Velasco, and C.W. Turck. 2015. The protein interactome of collapsin response mediator protein-2 (CRMP2/DPYSL2) reveals novel partner proteins in brain tissue. *Proteomics Clin. Appl.* 9:817–831. http://dx.doi.org/10.1002/prca.201500004

May, R.C., E. Caron, A. Hall, and L.M. Machesky. 2000. Involvement of the Arp2/3 complex in phagocytosis mediated by FcγR or CR3. *Nat. Cell Biol.* 2:246–248. http://dx.doi.org/10.1038/35008673

Menzies, A.S., A. Aszodi, S.E. Williams, A. Pfeifer, A.M. Wehman, K.L. Goh, C.A. Mason, R. Fassler, and F.B. Gertler. 2004. Mena and vasodilator-stimulated phosphoprotein are required for multiple actin-dependent processes that shape the vertebrate nervous system. *J. Neurosci.* 24:8029–8038. http://dx.doi.org/10.1523/JNEUROSCI.1057-04.2004

Moreau, V., J.M. Galan, G. Devilliers, R. Haguenauer-Tsapis, and B. Winsor. 1997. The yeast actin-related protein Arp2p is required for the internalization step of endocytosis. *Mol. Biol. Cell.* 8:1361–1375. http://dx.doi.org/10.1091/mbc.8.7.1361

Nakamura, F., K. Kumeta, T. Hida, T. Isono, Y. Nakayama, E. Kuramata-Matsuoka, N. Yamashita, Y. Uchida, K. Ogura, K. Gengyo-Ando, et al. 2014. Amino- and carboxyl-terminal domains of Filamin-A interact with CRMP1 to mediate Sema3A signalling. *Nat. Commun.* 5:5325. http://dx.doi.org/10.1038/ncomms6325

Nelson, W.J., and W.I. Weis. 2016. 25 years of tension over actin binding to the cadherin cell adhesion complex: The devil is in the details. *Trends Cell Biol.* 26:471–473. http://dx.doi.org/10.1016/j.tcb.2016.04.010

Norris, A.D., L. Sundararajan, D.E. Morgan, Z.J. Roberts, and E.A. Lundquist. 2014. The UNC-6/Netrin receptors UNC-40/DCC and UNC-5 inhibit growth cone filopodial protrusion via UNC-73/Trio, Rac-like GTPases and UNC-33/CRMP. *Development.* 141:4395–4405. http://dx.doi.org/10.1242/dev.110437

Pasic, L., T. Kotova, and D.A. Schafer. 2008. Ena/VASP proteins capture actin filament barbed ends. *J. Biol. Chem.* 283:9814–9819. http://dx.doi.org/10.1074/jbc.M710475200

Pollard, T.D. 2010. A guide to simple and informative binding assays. *Mol. Biol. Cell.* 21:4061–4067. http://dx.doi.org/10.1091/mbc.E10-08-0683

Qiao, C., C. Wang, F. Jin, D. Zheng, and C. Liu. 2015. Expression of collapsin response mediator protein 1 in placenta of normal gestation and link to early-onset preeclampsia. *Reprod. Sci.* 22:495–501. http://dx.doi.org/10.1177/1933719114549847

Reinhard, M., K. Giehl, K. Abel, C. Haffner, T. Jarchau, V. Hoppe, B.M. Jockusch, and U. Walter. 1995. The proline-rich focal adhesion and microfilament protein VASP is a ligand for profilins. *EMBO J.* 14:1583–1589.

Rosslenbroich, V., L. Dai, S.L. Baader, A.A. Noegel, V. Gieselmann, and J. Kappler. 2005. Collapsin response mediator protein-4 regulates F-actin bundling. *Exp. Cell Res.* 310:434–444. http://dx.doi.org/10.1016/j.yexcr.2005.08.005

Rottner, K., B. Behrendt, J.V. Small, and J. Wehland. 1999. VASP dynamics during lamellipodia protrusion. *Nat. Cell Biol.* 1:321–322. http://dx.doi.org/10.1038/13040

Schindelin, J., I. Arganda-Carreras, E. Frise, V. Kaynig, M. Longair, T. Pietzsch, S. Preibisch, C. Rueden, S. Saalfeld, B. Schmid, et al. 2012. Fiji: An open-source platform for biological-image analysis. *Nat. Methods.* 9:676–682. http://dx.doi.org/10.1038/nmeth.2019

Scott, J.A., A.M. Shewan, N.R. den Elzen, J.J. Loureiro, F.B. Gertler, and A.S. Yap. 2006. Ena/VASP proteins can regulate distinct modes of actin organization at cadherin-adhesive contacts. *Mol. Biol. Cell.* 17:1085–1095. http://dx.doi.org/10.1091/mbc.E05-07-0644

Shih, J.Y., S.C. Yang, T.M. Hong, A. Yuan, J.J. Chen, C.J. Yu, Y.L. Chang, Y.C. Lee, K. Peck, C.W. Wu, and P.C. Yang. 2001. Collapsin response mediator protein-1 and the invasion and metastasis of cancer cells. *J. Natl. Cancer Inst.* 93:1392–1400. http://dx.doi.org/10.1093/jnci/93.18.1392

Shih, J.Y., Y.C. Lee, S.C. Yang, T.M. Hong, C.Y. Huang, and P.C. Yang. 2003. Collapsin response mediator protein-1: A novel invasion-suppressor gene. *Clin. Exp. Metastasis.* 20:69–76. http://dx.doi.org/10.1023/A:1022598604565

Skau, C.T., D.S. Courson, A.J. Bestul, J.D. Winkelman, R.S. Rock, V. Sirotkin, and D.R. Kovar. 2011. Actin filament bundling by fimbrin is important for endocytosis, cytokinesis, and polarization in fission yeast. *J. Biol. Chem.* 286:26964–26977. http://dx.doi.org/10.1074/jbc.M111.239004

Skoble, J., V. Auerbuch, E.D. Goley, M.D. Welch, and D.A. Portnoy. 2001. Pivotal role of VASP in Arp2/3 complex-mediated actin nucleation, actin branch-formation, and Listeria monocytogenes motility. *J. Cell Biol.* 155:89–100. http://dx.doi.org/10.1083/jcb.200106061

Suetsugu, S., H. Miki, H. Yamaguchi, and T. Takenawa. 2001. Requirement of the basic region of N-WASP/WAVE2 for actin-based motility. *Biochem. Biophys. Res. Commun.* 282:739–744. http://dx.doi.org/10.1006/bbrc.2001.4619

Suraneni, P., B. Rubinstein, J.R. Unruh, M. Durnin, D. Hanein, and R. Li. 2012. The Arp2/3 complex is required for lamellipodia extension and directional fibroblast cell migration. *J. Cell Biol.* 197:239–251. http://dx.doi.org/10.1083/jcb.201112113

Takaku, M., H. Ueno, and H. Kurumizaka. 2011. Biochemical analysis of the human ENA/VASP-family proteins, MENA, VASP and EVL, in homologous recombination. *J. Biochem.* 149:721–729. http://dx.doi.org/10.1093/jb/mvr029

Tang, V.W., and W.M. Brieher. 2013. FSGS3/CD2AP is a barbed-end capping protein that stabilizes actin and strengthens adherens junctions. *J. Cell Biol.* 203:815–833. http://dx.doi.org/10.1083/jcb.201304143

Vasioukhin, V., C. Bauer, M. Yin, and E. Fuchs. 2000. Directed actin polymerization is the driving force for epithelial cell-cell adhesion. *Cell.* 100:209–219. http://dx.doi.org/10.1016/S0092-8674(00)81559-7

Verma, S., A.M. Shewan, J.A. Scott, F.M. Helwani, N.R. den Elzen, H. Miki, T. Takenawa, and A.S. Yap. 2004. Arp2/3 activity is necessary for efficient formation of E-cadherin adhesive contacts. *J. Biol. Chem.* 279:34062–34070. http://dx.doi.org/10.1074/jbc.M404814200

Verma, S., S.P. Han, M. Michael, G.A. Gomez, Z. Yang, R.D. Teasdale, A. Ratheesh, E.M. Kovacs, R.G. Ali, and A.S. Yap. 2012. A WAVE2-Arp2/3 actin nucleator apparatus supports junctional tension at the epithelial zonula adherens. *Mol. Biol. Cell.* 23:4601–4610. http://dx.doi.org/10.1091/mbc.E12-08-0574

Wang, L.H., and S.M. Strittmatter. 1996. A family of rat CRMP genes is differentially expressed in the nervous system. *J. Neurosci.* 16:6197–6207.

Weber, K.L., R.S. Fischer, and V.M. Fowler. 2007. Tmod3 regulates polarized epithelial cell morphology. *J. Cell Sci.* 120:3625–3632. http://dx.doi.org/10.1242/jcs.011445

Weisswange, I., T.P. Newsome, S. Schleich, and M. Way. 2009. The rate of N-WASP exchange limits the extent of ARP2/3-complex-dependent actin-based motility. *Nature.* 458:87–91. http://dx.doi.org/10.1038/nature07773

Welch, M.D., and T.J. Mitchison. 1998. Purification and assay of the platelet Arp2/3 complex. *Methods Enzymol.* 298:52–61. http://dx.doi.org/10.1016/S0076-6879(98)98008-9

Welch, M.D., and M. Way. 2013. Arp2/3-mediated actin-based motility: A tail of pathogen abuse. *Cell Host Microbe.* 14:242–255. http://dx.doi.org/10.1016/j.chom.2013.08.011

Welch, M.D., A.H. DePace, S. Verma, A. Iwamatsu, and T.J. Mitchison. 1997. The human Arp2/3 complex is composed of evolutionarily conserved subunits and is localized to cellular regions of dynamic actin filament assembly. *J. Cell Biol.* 138:375–384. http://dx.doi.org/10.1083/jcb.138.2.375

Welch, M.D., J. Rosenblatt, J. Skoble, D.A. Portnoy, and T.J. Mitchison. 1998. Interaction of human Arp2/3 complex and the *Listeria monocytogenes* ActA protein in actin filament nucleation. *Science.* 281:105–108. http://dx.doi.org/10.1126/science.281.5373.105

Winkelman, J.D., C.G. Bilancia, M. Peifer, and D.R. Kovar. 2014. Ena/VASP Enabled is a highly processive actin polymerase tailored to self-assemble parallel-bundled F-actin networks with Fascin. *Proc. Natl. Acad. Sci. USA.* 111:4121–4126. http://dx.doi.org/10.1073/pnas.1322093111

Withee, J., B. Galligan, N. Hawkins, and G. Garriga. 2004. *Caenorhabditis elegans* WASP and Ena/VASP proteins play compensatory roles in morphogenesis and neuronal cell migration. *Genetics.* 167:1165–1176. http://dx.doi.org/10.1534/genetics.103.025676

Xu, W., Y. Ge, Z. Liu, and R. Gong. 2015. Glycogen synthase kinase 3β orchestrates microtubule remodeling in compensatory glomerular adaptation to podocyte depletion. *J. Biol. Chem.* 290:1348–1363. http://dx.doi.org/10.1074/jbc.M114.593830

Yang, C., and T. Svitkina. 2011. Filopodia initiation: Focus on the Arp2/3 complex and formins. *Cell Adhes. Migr.* 5:402–408. http://dx.doi.org/10.4161/cam.5.5.16971

Yarar, D., W. To, A. Abo, and M.D. Welch. 1999. The Wiskott-Aldrich syndrome protein directs actin-based motility by stimulating actin nucleation with the Arp2/3 complex. *Curr. Biol.* 9:555–558. http://dx.doi.org/10.1016/S0960-9822(99)80243-7

Yoneda, A., M. Morgan-Fisher, R. Wait, J.R. Couchman, and U.M. Wewer. 2012. A collapsin response mediator protein 2 isoform controls myosin II-mediated cell migration and matrix assembly by trapping ROCK II. *Mol. Cell. Biol.* 32:1788–1804. http://dx.doi.org/10.1128/MCB.06235-11

Yonemura, S., Y. Wada, T. Watanabe, A. Nagafuchi, and M. Shibata. 2010. α-Catenin as a tension transducer that induces adherens junction development. *Nat. Cell Biol.* 12:533–542. http://dx.doi.org/10.1038/ncb2055

Yu, H.H., M.R. Dohn, N.O. Markham, R.J. Coffey, and A.B. Reynolds. 2016. p120-catenin controls contractility along the vertical axis of epithelial lateral membranes. *J. Cell Sci.* 129:80–94. http://dx.doi.org/10.1242/jcs.177550

Yu-Kemp, H.C., and W.M. Brieher. 2016. Collapsin response mediator protein-1 regulates Arp2/3-dependent actin assembly. *J. Biol. Chem.* 291:658–664. http://dx.doi.org/10.1074/jbc.C115.689265